

THE HAGUE
UNIVERSITY OF
APPLIED SCIENCES



Realisation of a repump-laser system at 313 nm for laser
cooling of Be^+ ions in a Paul trap

Bachelor thesis
LaserLaB, Vrije Universiteit Amsterdam
Under supervision of dr. Vincent Barbé & Elmer Gründeman (MSc)

Thomas Wendel 18029221

June 2, 2022

Abstract

The goal of this thesis is achieving saturation intensity of 76.5 mW/cm^2 for $2S_{1/2}$ $F=1 - 2P_{1/2}$ $F = 2$ transition in singly-ionized beryllium ions (Be^+). By enlarging the optical power of a laser diode at 626.266 nm via a bow-tie cavity and converting to 313.133 nm using Second Harmonic Generation in a nonlinear crystal like BBO or LBO, the saturation intensity can be obtained. The BBO crystal is used because this type of crystal has a higher conversion efficiency with respect to a LBO crystal. For an optical power of 8 mW at 626.266 nm fed into the cavity, the amount of second harmonic light is on the order of 10 microwatts . To obtain a saturation intensity of 765 W/m^2 , approximately $10 \text{ }\mu\text{W}$ of 313 nm light must be concentrated to a circular symmetric beam profile with a beam radius of less than $55 \text{ }\mu\text{m}$. Since the crystals are fabricated in such a way that the phase-matching condition for 626 nm in the resonance cavity cannot be fulfilled, producing $10 \text{ }\mu\text{W}$ of second harmonic light remains a theoretical possibility.

Contents

1	Introduction	1
1.1	Project background	1
1.2	Doppler cooling	1
1.3	The dark state in singly-ionized Beryllium ions for cooling laser	2
1.4	The 626 nm light-emitting laser diode	2
1.5	Saturation intensity at 313 nm	3
1.6	The research goals for the repump laser system at 313 nm	3
2	The laser diode emitting 626 nm light	6
2.1	A Distributed Bragg Reflector laser	6
2.2	The laser diode properties	6
3	The beamshaping of 626 nm light from laser diode	10
3.1	Collimation & optical isolation	10
3.2	Reshaping the elliptical beam profile of the laser diode	11
3.3	The mode field diameter of the single mode fiber	13
3.4	Mode-filtering	14
3.5	Maintaining linear polarisation with the single mode PM-fiber	15
3.6	Cavity beam waist	17
4	Second Harmonic Generation to 313 nm	18
4.1	Hänsch-Couillaud	18
4.2	Phase matching in nonlinear crystals	20
4.2.1	Intracavity polarizer	22
4.3	Crystal axis	24
4.4	Characteristics of the cavity	27
4.4.1	Finesse	27
4.4.2	The free spectral range of the resonance cavity	27
4.4.3	The full width half maximum of the resonance cavity	29
4.4.4	Q-factor	29
4.4.5	The power enhancement by the resonance cavity	30
5	The characterisation of 313 nm light	32
5.1	Optical power at 313 nm	32
6	Conclusion and outlook	36
6.1	Conclusion	36
6.2	Outlook	36
	References	37
A	Code for analysing beamprofile	38

1 Introduction

1.1 Project background

Under the leadership of Prof. Dr. K.S.E. Eikema, the research group Quantum Metrology and Laser Applications: Ultrafast Laser Physics and Precision Measurements for Fundamentals of the VU University Amsterdam is conducting experimental research to test the theory of Quantum Electrodynamics (QED). QED describes the interaction between charged particles and the electromagnetic field [1]. Next to the verification of the theory of QED, the research group is also conducting research into natural constants such as the electron/proton mass-ratio and the Rydberg constant. The reason for this research is that these constants are required for testing the QED theory. The experiment carried out in the He^+ laboratory to validate the QED theory involves cooling Helium ions (He^+) with a laser and determining the energy levels within He^+ with high precision spectroscopy. The measured energy levels can be then compared with theoretical predictions and the answer can be drawn as to whether or not QED works for systems like He^+ .

However, cooling down He^+ directly with light is not feasible because of the energy which requires light at 32 nm to excite the He^+ from the 1S state to the 2P state. There is no continuous wave-source that can emit 32 nm and light at 32 nm cannot propagate through air. To cool down He^+ , sympathetic cooling is used with the help of singly-ionized beryllium ions (Be^+). Beryllium⁺ has one valence electron in the 2S state. Due to a missing electron in the 2S state, positive net charge enables the atoms to exert force on one another also known as the Coulomb-force. This force is used to sympathetically cool He^+ . Additionally, the energy structure in Be^+ is more favourable, because lower energies (≈ 313 nm) are required in order to cool down Be^+ . Furthermore, beryllium is an atom with a mass closest to that of helium, making it the most suitable for sympathetic cooling.

1.2 Doppler cooling

The fact that light can exert a force on atoms is the basis for laser cooling. Doppler cooling is a type of laser cooling that uses the Doppler effect to lower atoms kinetic energy by adjusting the laser frequency below the atoms transition frequency. Only atoms travelling towards the laser source with enough momentum to overcome the energy gap (due to the Doppler effect) of the red shifted laser will be cooled in this setup. When an atom absorbs a photon and transitions to an excited state, it loses momentum equivalent to the photon's momentum. If the atom relaxes to its ground state again, it will emit a photon in a random direction with a transition energy equal to the transition energy. Over many transition cycles, the momentum of the absorbed photons add up while the average momentum of the emitted photons is zero.

The 313 nm transition in Be^+ is fast-cycling: it has a 19.4 MHz linewidth which means that one can scatter many laser-cooling photons at μs timescale and thus cool down very fast. Also it can be used as a fluorescence detection transition: Upon 313 nm radiation irradiation, Be^+ will absorb and re-emit many 313 nm photons over a small timescale which allows rapid detection of the ion by the detection of the emitted fluorescence photons.

Atoms ideal for laser cooling, on the other hand, are never real two-level systems. As a result, an excited atom may decay to a state other than the cooling transition's groundstate, sometimes referred to as a dark-state. The cooling transition for Be^+ is between $2\text{S}_{1/2}$ - $2\text{P}_{3/2}$ states. .

1.3 The dark state in singly-ionized Beryllium ions for cooling laser

The dark state for Be⁺ in the He⁺ experiment is $2S_{1/2}$, $F = 1$ state. The cooling laser that is used for the $2S_{1/2}$, $F = 2$, - $2P_{3/2}$ transition (cooling transition) cannot cover the detuning of 197 GHz ($\Delta\nu_{FS}$ in figure 1) between the $2P_{1/2}$ and the $2P_{3/2}$ states. Therefore, a separate laser system is required to repump the ion back from the dark state transition ($2S_{1/2}$, $F = 2$ - $2P_{1/2}$) to the cooling transition ($2S_{1/2}$ - $2P_{3/2}$). The repump transition does not directly cause the ion to return to the cooling transition, but causes the ion to enter the $2P_{1/2}$ state after which the ion can decay in various routes, including back to the cooling transition. The repump transition from the $2S_{1/2}$ - $2P_{1/2}$ is advantageous for sub-doppler cooling.

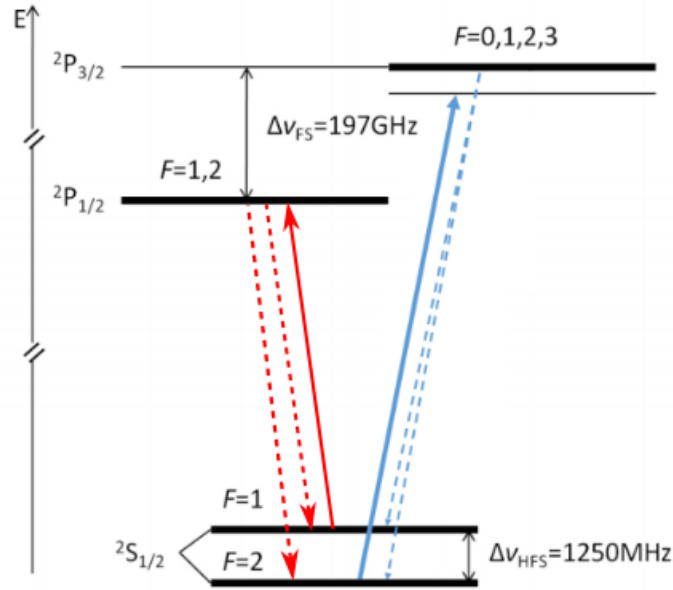


Figure 1: The cooling transition (thick blue line) and its possible decay routes (Blue striped lines). One of the possible decay routes is into the $2S_{1/2}$, $F = 1$ state. This state is a so called 'dark state' for the cooling laser. Therefore, a new laser system is build to repump the beryllium ions from the $2S_{1/2}$, $F = 1$ state to the $2P_{1/2}$ (Red thick line). From there the ion can decay back into the cooling transition (Left-sided red striped line) without interfering with the doppler cooling.

1.4 The 626 nm light-emitting laser diode

High power laser systems at 313 nm exist, using infrared lasers and Sum Frequency Generation and Second Harmonic Generation to get 313 nm light. However, these setups are relatively large and expensive and amount of light in these setups is more than required for this purpose. The small amount of light that is required can be easily achieved by using a laser diode emitting 626 nm light and use Second Harmonic Generation to achieve 313 nm light. The Ferdinand-Braun institut in Berlin designed a Distributed Bragg Reflector (DBR) ridge waveguide laser which is able to output more than 50 mW at 626.0 nm, while internally cooled to 0° [2]. The spectrum width is less than 1 MHz, which is suitable for all applications using beryllium ions.

The 626 nm light (fundamental) can be converted to 313 nm (harmonic) with Second Harmonic Generation (SHG) inside non linear crystals like Barium Borate (BBO or β -BaB₂O₂) and Lithium Borate (LBO or Li₂B₄O₇). SHG is not an efficient process and scales non linearly with the fundamental power. More fundamental power gives higher efficiency. Therefore, as much power for the fundamental light is required. A bow-tie resonance cavity will be used for enhancing the fundamental light since the laser diode

can only deliver up to 50 mW at 626 nm. The bow-tie resonance cavity is designed by F.M.J. Cozijn and it has already been proven that the design works.

The wavelength emitted by the laser diode can be tuned by changing the temperature in the laser diode. The tuning is necessary to set a wavelength of 626.266 nm with a temperature controller. Frequency doubling this wavelength gives a 313.133 nm wavelength, what corresponds to the repump transition frequency.

1.5 Saturation intensity at 313 nm

The linewidth for the repump transition from 2S_{1/2} to 2P_{1/2} in Be⁺-ions is $2\pi \times 18$ MHz according to the NIST atomic database [3]. The name linewidth and lifetime can be used interchangeably. The lifetime means an amount of time before the atom is excited once and returns to its ground state. The lifetime of 2P_{1/2}-state in Be⁺ is approximately 8.9 ns. The excitation requires photons at 313.133 nm. Calculate the saturation intensity (equation 1) to prevent the constraint in transition frequency caused by a lack of photons.

$$I_{sat} = \frac{\pi \cdot h \cdot c \cdot \gamma_{313.133nm}}{3 \cdot \lambda_0^3} \quad (1)$$

I_{sat} is the saturation intensity, also know as the intensity at which the photons do not further limit the transition rate, h is Planck's constant ($6.626176 \cdot 10^{-34}$ Joule·Hz⁻¹), c is the speed of light (299792458 m·s⁻¹), $\gamma_{313.133}$ is the scatter rate for this transition ($2\pi \times 18$ MHz) and λ_0 is the specific wavelength for this transition (313.133 nm). Filling these in for equation 1 gives an saturation intensity of approximately 76.5 mW/cm² (764.59 W/m²).

The spot size is not one square meter, rather in the magnitude of μ m. The radius of the light beam is estimated at 50 microns at the most. The required optical power at 313.133 nm can be determined by assuming that the beam profile is circular. Equation 2 can be filled in to obtain the required optical power at 313 nm.

$$P_{313nm} = I_{sat} \cdot \pi r^2 \quad (2)$$

The radius at 50 micron gives an optical power of 6 μ W. Therefore, very little amount of optical power at 313 nm is sufficient to saturate the 2S_{1/2} - 2P_{1/2} transition in Be⁺-ions. However, the radius is not fixed and can still vary. The required optical power at 313 nm as function of the beam radius is depicted in figure 2.

1.6 The research goals for the repump laser system at 313 nm

The aim of this project is to achieve the saturation intensity of 765 W/m² for the 2S_{1/2} - 2P_{1/2} transition in Be⁺-ions. Can the saturation intensity of 76.5 mW/cm² for the 2S_{1/2} - 2P_{1/2} at 313.133 nm in singly-ionized Be⁺-ions be reached with resonance cavity enhanced light at 626.266 nm and converted to 313.133 nm by Second Harmonic Generation in BBO or LBO crystals?

The optical power at 313 nm is in the order of micro watts. This is a very small amount, but the project should show whether this order size for optical power is feasible. Therefore, research questions can be set up to ensure the project goals is reached.

First, the distributed Bragg Reflector laser diode is a device which can be temperature tuned to set the emitted wavelength. The questions therefore is: Can the wavelength emitted by the laser diode set to 626.266 nm, that the frequency doubled light is 313.133 nm? Additionally, what are the settings for the temperature- and diode controller at

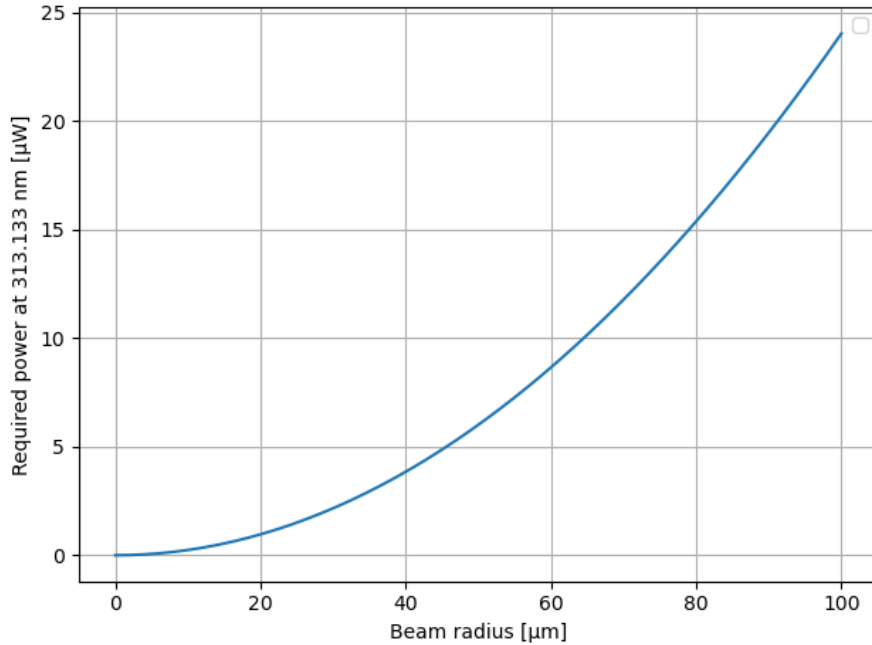


Figure 2: The required optical power at 313 nm as function of the beam radius assuming the beam profile is circular and symmetric. This plot is made with equation 2 with a fixed saturation intensity at 765 W/m^2

626.266 nm if this specific wavelength is achieved? Since the laser is a diode, is the beam profile emitted by the laser diode circular and is the intensity distribution an estimated Gaussian? A program called GaussianBeam will be used to simulate the Gaussian beam propagating through the setup.

The 626 nm light from the laser diode is enhanced in a resonance cavity, because the maximum amount of optical power emitted by the laser diode is 50 mW. This amount of power (50 mW) is too low for a single pass through a non linear crystal. By using a resonance cavity, 626 nm light will pass many times through the crystal, resulting in more conversion and therefore more 313 nm light. What is the power enhancement of the cavity? Is the conversion to 313 nm sufficient as result of 626 nm power enhancement? What are finesse, FWHM and the Free spectral range of this resonance cavity? How are the optical axis oriented inside the BBO- and LBO crystals? Are the crystals produced that the light can achieve phase matching inside the cavity?

Lastly, if there is 313 nm produced by Second Harmonic Generation inside the cavity, how much power is there at 313 nm? Is this amount enough to saturate the $2S_{1/2} - 2P_{1/2}$ transition in Be⁺? Does the 313 nm light need beam shaping?

The lab already has all of the components needed to build this repump laser system. This thesis will not include any component design. However, in this thesis, thoughts on how the set-up will look are covered. The most significant limitation is the amount of space that this repump laser system can occupy. The repump laser system can only take up a surface of 55 x 45 cm and the surface cannot be extended any further. A schematic of the setup produced for achieving 313 nm light is depicted in figure 3

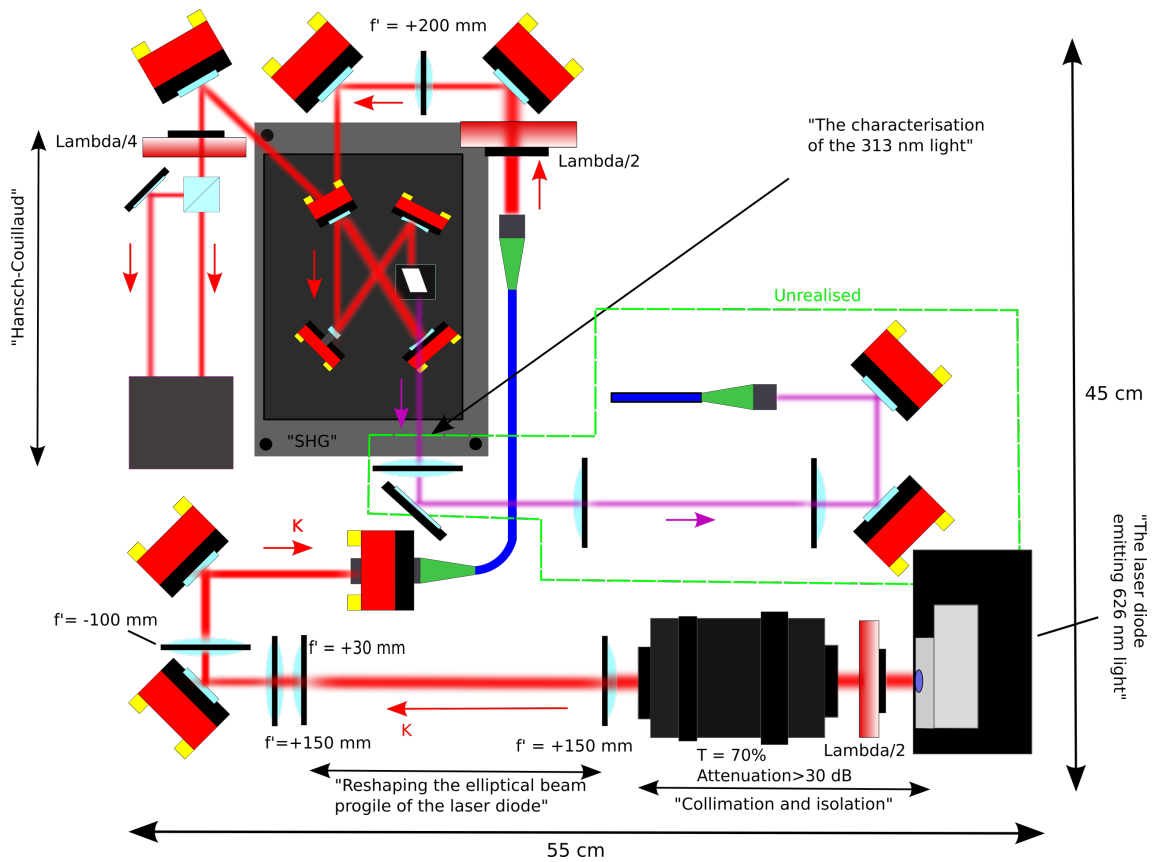


Figure 3: A schematic of the setup produced. The laser diode emits 626 nm light (bottom right corner) which then propagates through the telescopes and fiber. The light gets injected into the cavity, which is locked with a Hansch-Couillaud locking scheme.

2 The laser diode emitting 626 nm light

A laser diode is a turn key device which can deliver high amounts of optical power with specific wavelengths. This chapter will describe a distributed Bragg reflector (DBR) laser diode [?] which will be used to create light at 626 nm for Second Harmonic Generation (SHG) to 313 nm since there is no laser diode that can directly emit 313 nm. Furthermore, this chapter will describe how the diode lases and how the wavelength can be set by the temperature and current inside the laser diode. Lastly, the beam profile will be discussed as it is important for the resonance cavity and SHG.

2.1 A Distributed Bragg Reflector laser

A distributed Bragg Reflector (DBR) diode laser is made up of a normal ridge waveguide diode laser with an incorporated grating that works as a wavelength selector. As a result, in an extended cavity laser configuration, an external wavelength selecting element such as a grating is avoided. This has the tremendous benefit of being able to fit the entire structure inside the diode package and being intrinsically stable due to the monolithic structure. As a result, it is relatively insensitive to vibrational disturbances and possibly wavelength selective element misalignment issues.

2.2 The laser diode properties

The wavelength is mainly dependent on the temperature of the laser diode. Since the wavelength must be specifically 626.26 nm (313.133 nm after frequency doubling required for optical repumping of Be^+), it is necessary to check which temperature corresponds to this wavelength. In figure 4 the wavelengths are displayed as function of the temperature of the laser diode. Looking for a wavelength close to 626.26 nm gives a temperature around 5 °C according to the graph. The specific temperature has to be found for setting the emitted wavelength at 626.26 nm. Tuning the temperature can be done by changing the current of the peltier element. The temperature is measured by measuring the resistance of a thermistor (10K3CG NTC thermistor) inside the laser diode.

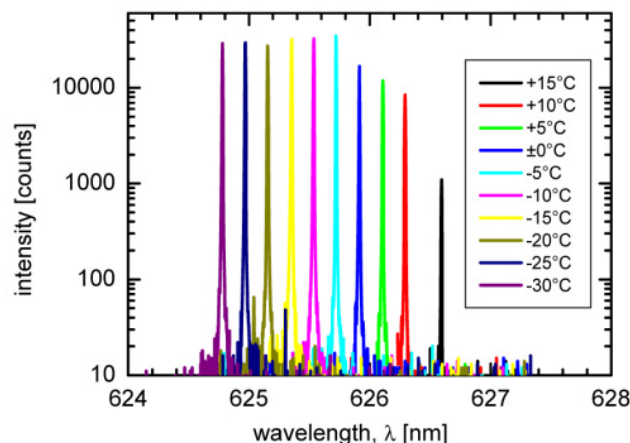


Figure 4: *The lasing intensity as function of wavelength at specific temperatures. The smallest wavelength (peak on the left) corresponds to the lowest temperature. The intensity per wavelength decreases as the temperature increases because of the mismatch between the grating and the peak of the gain spectra. The third peak from the right corresponds to 5 degree Celsius. Taken from [2]*

The 626.26 nm wavelength is found by connecting the laser diode via a fiber to a wavemeter (WSU-30) and by tuning the temperature of the peltier with a temperature controller (TED200C). The resistance of this specific thermistor is 26.17 ± 0.02 k Ω . The value for

the resistance is measured, which corresponds to 4.5 ± 0.1 °C for a wavelength of 626.26 ± 0.01 nm.

The optical power emitted by the laser diode is temperature dependent because the optical power is dependent on the wavelength selection in the grating and the peak of the gain spectra. A mismatch between the spacing of the grating and the peak in gain spectrum causes a loss in optical power. The grating spacing increases for increasing temperature, so the mismatch increases and therefore cause a drop in optical power while at lower temperatures the peak in the gain spectra is closer to wavelength of operation. This can be observed in figure 5. Since the temperature is close to 5 °C, the green line (third line on the right) represents the optical power output for the laser diode. The diode controller (LDC200C) has a maximal current output of 100 mA, so the maximal optical power output for the laser diode at a temperature of 4.5 ± 0.1 °C and 100 mA current is around 15 mW.

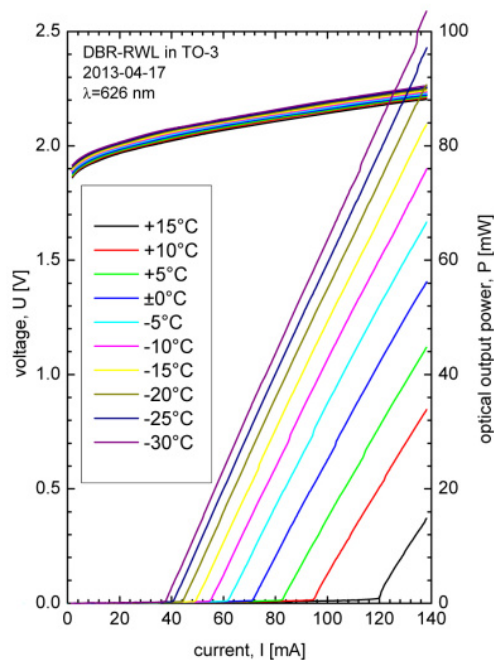


Figure 5: The optical power (right y-axis) as function of the laser diode current (x-axis). The lines that run from the x-axis to the right y-axis belong to this coordinate system. The third line on the right (green) is around the used temperature for the laser diode and therefore represents the optical power output of the laser diode. The lines at the top of the graph are not important as it only the voltage (left y-axis) as function of the current. Taken from [2]

The maximal optical power output for the laser diode at 4.5 ± 0.1 °C can be verified by measuring the optical power as function of current sent through the laser diode. Figure 6 shows an measurement of the optical power output of the laser diode at a temperature of 4.5 ± 0.1 °C. The current on the x-axis is increased with steps of 5 mA as the optical power is on the y-axis. The error bars for the optical power include the stray light from the laboratory and the uncertainty of the power meter. The error bars for the current are set by the specifications for the diode controller which is so small it cannot be seen in the graph.

The spectra peaks in figure 5 can be plotted as function of temperature, represented by the black squares in figure 7. According to [?] the slope of the black line is 0.039 nm K⁻¹. The red dots depict the diode laser's free-running wavelength spontaneous emission if the DBR is absent, demonstrating that the DBR can adjust the wavelength by up to 5 nm. While the DBR-temperature RWL's allows for coarse wavelength adjustment, fine

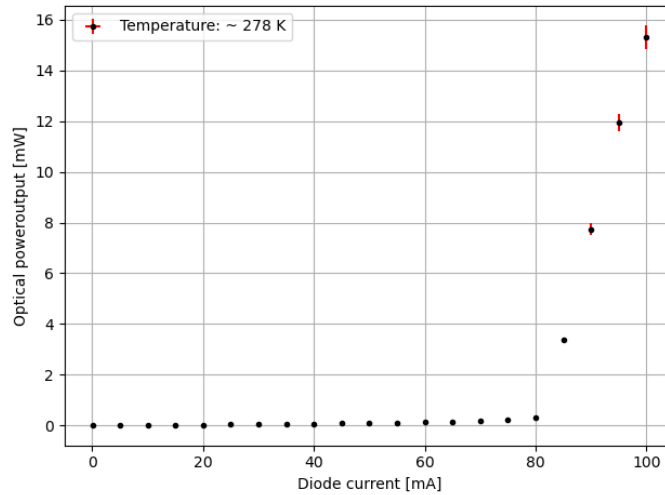


Figure 6: Measurement of the optical power output as function of the diode current. The temperature in the laser diode is 4.5 ± 0.1 °C. This temperature corresponds to a emitted wavelength

tuning is done with the diode driving current, which has a tuning rate of roughly 0.74 pm mA⁻¹. To facilitate narrowband functioning, both temperature and current must be suitably stabilized. The laser diode has a linewidth of about 1 MHz at 120 mA and 0 °C.

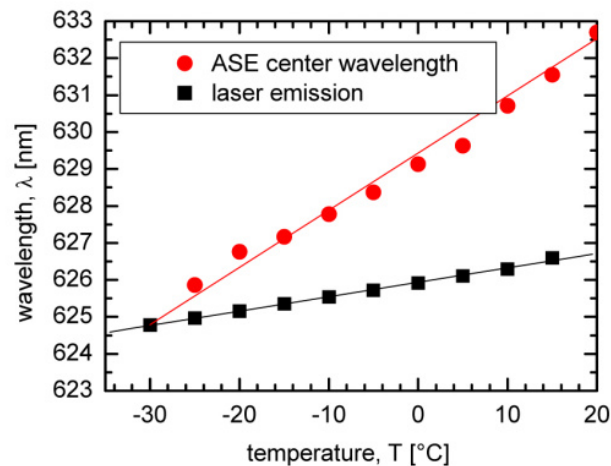


Figure 7: Spectral center positions of the increased spontaneous emission (red dots) and the lasing emission as a function of temperature (black squares). Taken from [2]

Characteristics such as wavelength due to temperature and current and their effect on optical power have been discussed. Additionally, one of the characteristics of the laser diode that has not been discussed is the beamprofile of the laser diode. The beamprofile is elliptical due to the geometry of the laser diode. The rectangular shape of the diode's active region causes different divergence angles in the horizontal and vertical axes as shown in figure 8.

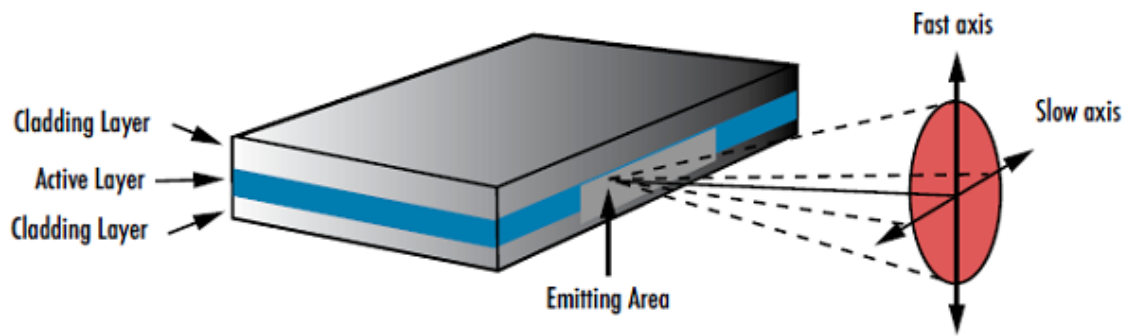


Figure 8: *Schematic of the laser diode emitting light with an elliptical beamshape due to difference in diffraction in two directions. Image taken from [4]*

The light from the laser diode needs to be coupled in to a resonance cavity where the light can build up power for SHG. The beam profile needs to have a 2-D Gaussian intensity profile for high incoupling efficiency. Therefore, the elliptical beamprofile needs to be reshaped to obtain this Gaussian beam profile. The intensity distribution can be 2-D Gaussian even if the beam profile is not 2-D Gaussian. The next chapter will discuss beam shaping of 626 nm light for high incoupling efficiency into the resonance cavity.

3 The beamshaping of 626 nm light from laser diode

The previous chapter explained how the laser diode works, the propagation of light from the diode and the beam profile. This chapter describes how the beam profile can be matched to the resonance cavity. By filtering out the higher transverse modes, one can obtain only the TEM₀₀ mode which can be approximated by a Gaussian intensity distribution. A Gaussian intensity distribution can be achieved by using telescopes to adjust the shape and size of the beam profile for fiber injection and using a single mode fiber to obtain only the fundamental mode which provides the Gaussian distribution.

3.1 Collimation & optical isolation

Optical losses due to divergence of the light beam can be minimised by collimating the light. Also, light collimation simplifies adjusting the shape and size of the beamprofile. This setup makes use of Thorlabs' A390TM-A aspheric lens to collimate the light emitted by the laser diode. Furthermore, optical feedback to the laser diode is prevented by isolating the light using a Faraday isolator (Gsänger Faraday isolator 500-820 nm). The optical isolation is depicted in figure 9. There are two polarisation beamsplitter cubes next to a Faraday rotator. The Faraday rotator together with 2 polarisation beamsplitter cubes is what is called a Faraday isolator. To have the highest transmission through the Faraday isolator, one has to match the incoming light polarisation with the transmission polarisation of the input beamsplitter. Therefore, a $\frac{\lambda}{2}$ waveplate (WPH05M-633) is placed in front of the input-polarisation beamsplitter cube of the Faraday isolator.

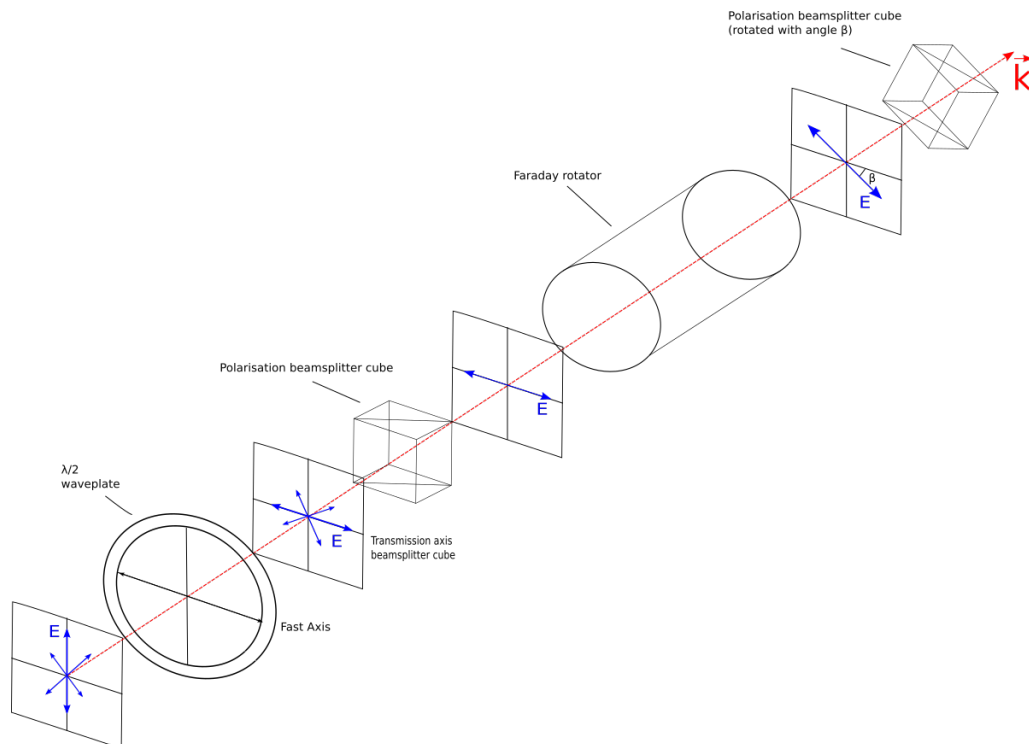


Figure 9: From left to right: Different oriented linear polarised light is incident on the $\frac{\lambda}{2}$ waveplate. The waveplate is rotated such that most of the linear light is transmitted through the input polarisation beamsplitter cube. Light, with a polarisation other than the transmission polarisation of the input beamsplitter cube, gets reflected. The linear polarisation acquires an angle β , which is 45° after transmission through the rotator.

However, not all light that is emitted by the laser diode is linear polarised light. The waveguide in the laser diode acts as a polariser, hence lasing occurs at one specific polarisation. However, spontaneously emitted photons can have different polarisations.

the WPH05M-633 ($\frac{\lambda}{2}$ -waveplate) is not designed for 626 nm, which means that not all the light will be linearly polarised according to the waveplate's polarisation direction. This will cause a loss of optical power when transmitted through the optical isolator, because the light's polarisation is not aligned with the transmission polarisation of the cube. An improvement for the setup would be using a waveplate that is designed for 626 nm. An optical power measurement before and after the isolator is used to determine the transmission through the isolator. In this case, the measured reflection attenuation is more than 30 dB for measured transmission of $\sim 70\%$ at 626 nm. According to the specifications, guaranteed attenuation is 30 dB for a $\sim 90\%$ transmission (design wavelength). Although this optical isolator is not designed for 626 nm, the attenuation is consistent with the specifications.

3.2 Reshaping the elliptical beam profile of the laser diode

The beam profile emitted by the laser diode is not suitable for the resonance cavity due to the beam profile- and size. The camera that is used for looking at the beamprofile is a Manta G235-B camera which has a pixel size of $5.86 \mu\text{m}$. Additionally, Vimba software is used to read out the camera and manage camera setting such as gain and shuttertime. The laser diode emits a beam of elliptical beam profile as shown in figure 10, which cannot be directly injected into the resonance cavity because the fundamental TEM₀₀ of the bow-tie resonance cavity is rotationally symmetric. Therefore, beamshaping is required to eliminate ellipticity. The images do not have a system of axes. The shape of the beam is discussed in terms of horizontal and vertical. In this case, horizontal is from left to right and vertical is from top to bottom.

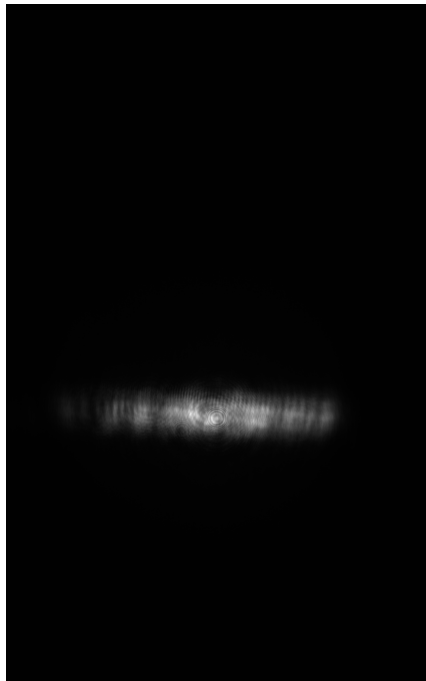


Figure 10: *The beamprofile emitted by the laser diode. The pattern can be from the higher modes, diffraction or interference in between optical attenuation plates, which were required to prevent camera saturation. Picture is taken with a Manta G235-B camera and Vimba software.*

Reshaping the beamprofile in to a circular profile can be done with a telescope using cylindrical lenses. Cylindrical lenses are lenses that only focus light in one axis of choice. In the case described in figure 10, the first positive lens is used to focus the collimated light horizontally. Additionally, the second lens is required to collimate the light after focusing.

First, creating the telescope requires horizontal magnification. The magnification between

object and image is given by [5]:

$$M = \frac{-f_o}{f_e} \quad (3)$$

Where M is the magnification of the telescope, f_o is the focal length of the objective lens and f_e the focal length of the ocular lens. The ratio between the height and width of the beam can be determined by taking a picture of the beam and having a software program determine the dimensions of the width and height. The analysis software was made by Dr. M. Collombon.

This software gives the Full Width Half Maximum (FWHM) and the waist ω_0 . The waist is defined as the distance from the center of the beamprofile where the intensity is decreased with $\frac{1}{e^2}$ and this will be used for this thesis. Additionally, the definition of the beam diameter is $2\omega_0$. Figure 11 shows the analysis of figure 10. The software does not give any uncertainties about the dimensions of the FWHM and waist. The interface does not return an uncertainty in the FWHM and the waist of the fit.

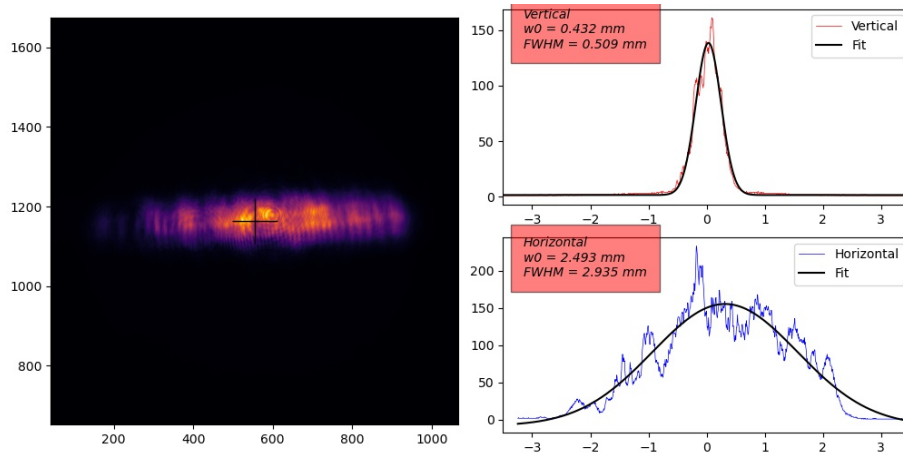


Figure 11: *Left: picture of the beam profile with intensity distribution. Right: The analysing of the beamprofile on the left. The beamprofile is elliptical because the horizontal waist is bigger then the vertical waist.*

The vertical waist is 0.432 mm. The horizontal waist of the beam is 2.493 mm and is 5.77 times bigger than the vertical waist of the beam profile. Since the size of the uncertainty is not known, the ratio is estimated to be 6 times bigger. To give this beam profile a circular shape, it can be said that the telescope required must either increase the vertical waist or reduce horizontal waist by a factor of 6. In this arrangement, the choice is made to reduce the horizontal waist by 6 times. The reason for this is that the light has to be coupled in an optical fiber, for which the beam profile should not be too large to match the collimator aperture and give correct spot size at the focus of the collimator. The latter is required to match roughly the LP₀₁ mode in a single mode fiber, which will be described in section” 3.3.

However, there is no combination of available lenses within the lab with a magnification factor of 6. Therefore, using formula 3 the combination of lenses with 5x magnification is chosen. In addition, it should be a compact telescope to save space and the combination must be easily achieved with available lenses. In this setup, planoconvex cylindrical lenses with $f_o = +150$ mm and $f_e = +30$ mm are selected. The length of the telescope is set by the combined focal lengths of the lenses, so this telescope is 180 mm or 18 cm in length. It is possible to use f_e is -30 mm to create a more compact telescope, but at the time of writing the thesis this was not present in the lab.

The beam profile after propagation through the telescope is depicted in figure 12. There is a slight ellipticity in the beam profile because the lens combination in the telescope is not magnifying with a factor of 6x and because of astigmatism.

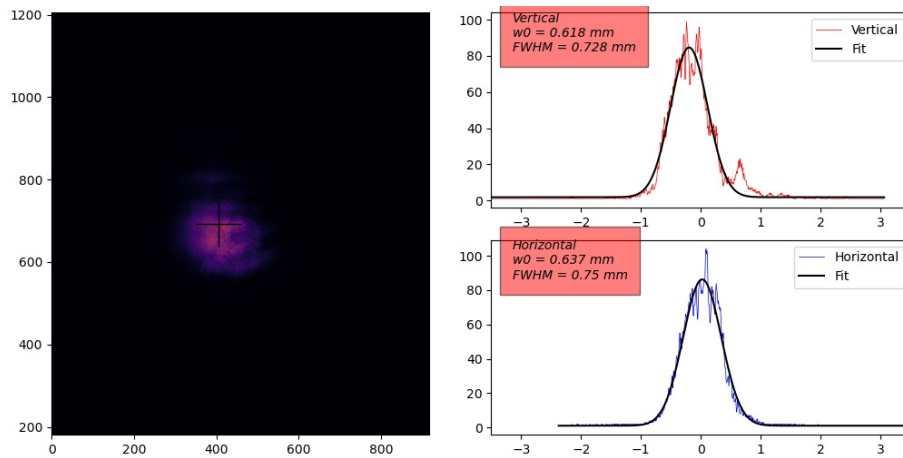


Figure 12: *Beam profile after propagation through the 180 mm telescope used for eliminating ellipticity. The beam is close to circular. The beam profile as in this image is sufficient to build on.*

This beam profile is circular enough to be coupled into a single mode fiber. However, the cross which indicates the fit center is not in the middle of the spot. In this case, it is not an issue since the beam profile looks mostly circular.

Paragraph 3.3 will describe the determination of a second telescope which is required to match the incoming light beam diameter with the mode field diameter of the fiber after focussing in the collimator.

3.3 The mode field diameter of the single mode fiber

The mode field diameter (MFD) describes the width of the intensity profile along a single mode fiber. This MFD is essential for obtaining the optimal focus diameter for maximum light coupling efficiency. The beam waist as shown in figure 12 is around 0.62 mm for the vertical waist and around 0.63 mm for the horizontal waist. The fiber in this setup is a polarization-maintaining fiber from Thorlabs (P3-630PM-FC-1) and the polarization-maintaining part will be described in section 3.4. The MFD for this specific fiber is $4.5 \pm 0.5 \mu\text{m}$ at 630 nm.

The fiber collimator (Schäfter+Kirchoff 60FC-4-A4.5S-02) is equipped with a lens with a focal length of 4.5 mm that can be moved inside the collimator. This is useful for optimising transmission through the fiber. Since the focal length and the beam waist are known, one can compute the waist at the focus after the lens. The focus diameter ($2w$) has to match the MFD for maximal incoupling efficiency. Computing this situation in GaussianBeam gives a focus waist of around $1.5 \mu\text{m}$.

Since the focus waist of $1.5 \mu\text{m}$ is smaller than the half of the MFD ($2.25 \mu\text{m}$), light can be coupled in. However, it is more sensitive for alignment. Therefore the focus diameter has to be enlarged to counter possible alignment issues. To match the MFD, the focus has to be increased with a factor of 1.5. Consequently, the beam waist before the collimator (before focussing) has to decrease with a factor of 1.5. This means that the $600 \mu\text{m}$ waist has to be decreased to a waist of $400 \mu\text{m}$.

A second telescope is therefore used to decrease the waist from $600 \mu\text{m}$ to $400 \mu\text{m}$. Since this is a factor of 1.5, so must the ratio between lenses in the telescope be 1.5. With the lenses available in the lab, a telescope is built using one planoconvex lens with $f_o = +150$

mm and one planoconcave lens with $f_e = -100$ mm. The total length of this telescope is 50 mm. Figure 13 shows the situation with both telescopes in the setup.

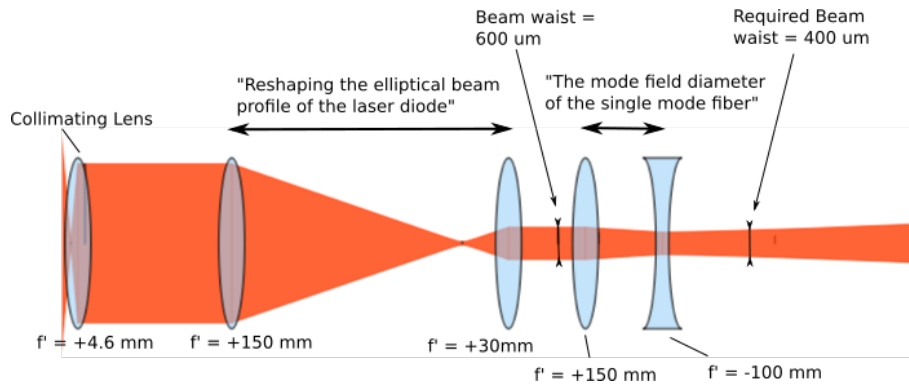


Figure 13: *From left to right: Light propagation from the laser diode with the collimating lens. After the telescope described in "Reshaping elliptical beam profile" the waist is $600 \mu\text{m}$. By using a telescope that has a 1.5 times magnification one can decrease the beamwaist from $600 \mu\text{m}$ to $400 \mu\text{m}$. The beamwaist of $400 \mu\text{m}$ is required for optimal incoupling efficiency into the fiber*

3.4 Mode-filtering

The laser diode emits other transverse (TEM) modes besides the TEM_{00} mode. A transverse mode of electromagnetic radiation is a specific electromagnetic field pattern of the radiation in the plane perpendicular (i.e., transverse) to the propagation direction of the radiation. The TEM_{00} mode is providing the Gaussian intensity distribution and is desired for the resonance cavity. For this reason other TEM modes must be suppressed and only the TEM_{00} mode must remain. One can use a single mode fiber to suppress the other TEM modes. Additionally, the fiber must maintain the polarisation (subsection 3.5) because the cavity only accepts one certain polarisation which will be discussed in paragraph 4.2.

This setup makes use of polarisation maintaining (PM) single mode fiber P3-630PM-FC-1 from Thorlabs. As described previously, the fiber collimator Schäfter+Kirchoff (60FC-4-A4.5S-02) is used to couple the light into the fiber. The fiber is 1 meter long and has a panda stress-rod configuration. Figure 14 shows a cross-section of a PM fiber with a panda stress rod configuration as used in the setup. Additionally, "PANDA" stands for Polarization-maintaining AND Absorption reducing [6].

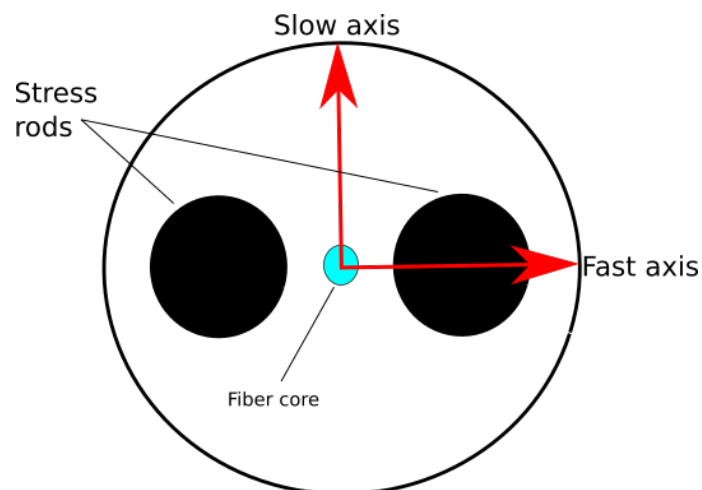


Figure 14: *Cross-section of a PM fiber with the panda stress rod configuration. The stress rods apply a force on the fiber core which causes systematic linear birefringence in the fiber core.*

3.5 Maintaining linear polarisation with the single mode PM-fiber

Isotropic materials are not birefringent. By inducing mechanical stress on a isotropic material, isotropic material becomes anisotropic and therefore birefringent. By creating the birefringence in the fiber core, one can split up the indices into a fast and slow axis. The name of the axis are set by the refractive index in this axis because the speed of light through a medium is defined by the speed of light divided by the refractive index of a material. So if a material is birefringent, the speed of light through this medium can have two different velocities depending on the light polarisation.

The light coming out of the isolator is linearly-polarized and its direction of polarization has to match one of the two neutral axis of the fiber to achieve polarisation-maintaining. Matching one of fiber neutral axis with the transmitted light can be done by either using a $\frac{\lambda}{2}$ waveplate or by rotating the fiber until polarisation is maintained. The matching of the axis is chosen to be done by rotating the fiber, because this takes less time and will be less expensive than ordering a new waveplate. Figure 15 shows the matching of one neutral axis with the polarisation of the light.

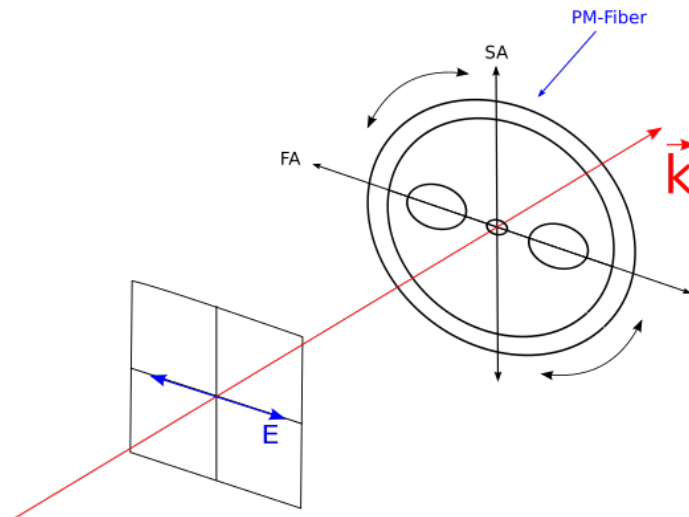


Figure 15: The neutral axis of the PM-fiber can be met by rotating the fiber with respect to the polarisation direction of the incoming light.

The fiber is polarisation maintaining with a 5 % error. This means that when the fiber gets heated or moved, 5 % of the light is leaving the fiber with another polarisation direction than the incoming polarisation. This 5% error is measured by looking at the polarisation at the end of the fiber using an polarising beamsplitter cube. By putting a photodiode after the polarising beamsplitter cube, one can measure the transmitted polarisation of the beamsplitter cube. Twisting and heating the fiber causes a loss in transmission through the beamsplitter cube because if the incoming light onto the fiber is not matched with one of the neutral axis, light with a different polarisation is transmitted through the fiber and is not transmitted through the beamsplitter cube.

Due to reflections and losses in the fiber or optical power that is manifested in higher order modes, transmission through a fiber never reaches 100 %. For instance, one can state that optical power is stored in higher order TEM modes which causes to have less optical power in the TEM₀₀ mode. Therefore, when higher order modes are filtered from the incoming beam, one can observe a drop in optical power. Additionally, another reason can be the alignment of the two telescopes. Manipulation of the beam profile can result in a loss of optical power if the beam profile is not perfectly round or is not the right size for the mode field diameter. The total transmission for the fiber is 56 % with the assumption that it remains constant over time. This is sufficient for incoupling since the cavity will be enhancing this power.

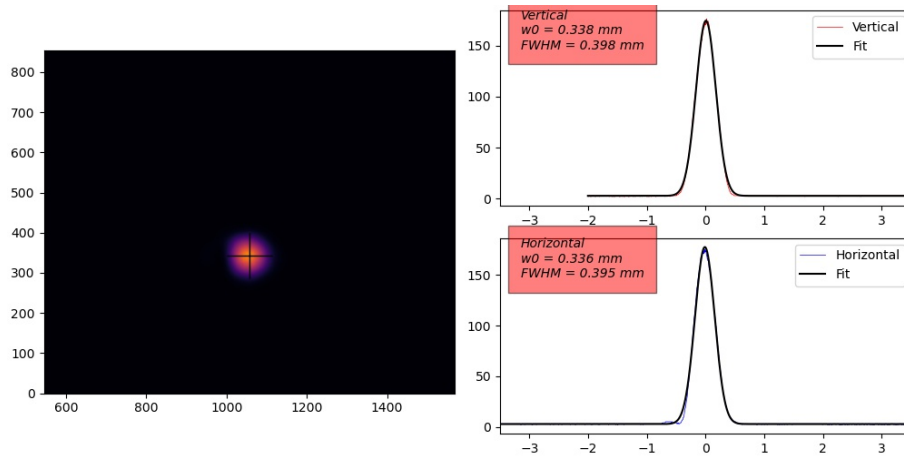


Figure 16: *Cross-section of the beam after the single mode fiber and the fiber collimator. The beam is slightly focussed, but the beam was collimated this image. The waist is around 400 μm and not around 300 μm as in this image. This image is for illustration purposes. Picture taken from a 20 cm distance from the fiber.*

Another fiber collimator (CFC-8X-A) is connected on the back-end of the single mode fiber. This fiber collimator ensures that the light is collimated once it leaves the fiber. Checking if the light is collimated and not focussed, one can look in the far field. The expected beam waist from the fiber is 400 μm .

To check if the beamprofile is improved by transmission through the fiber, images are made with the Manta camera. Figure 16 shows an cross-section of the beamprofile produced by the single mode PM fiber.

3.6 Cavity beam waist

The resonance cavity best accepts monochromatic light with a focus spot in the cavity where the beamwaist ω_{focus} equals $100 \mu\text{m}$ [7]. For a slight focus, a lens with a large focal length can be used to focus the light into the cavity. The position of this slight focus will be further discussed in chapter 4, but for now the focus must be in front of the second mirror inside a bow-tie cavity. Figure 17 illustrates the cavity to show the position of the focal spot.

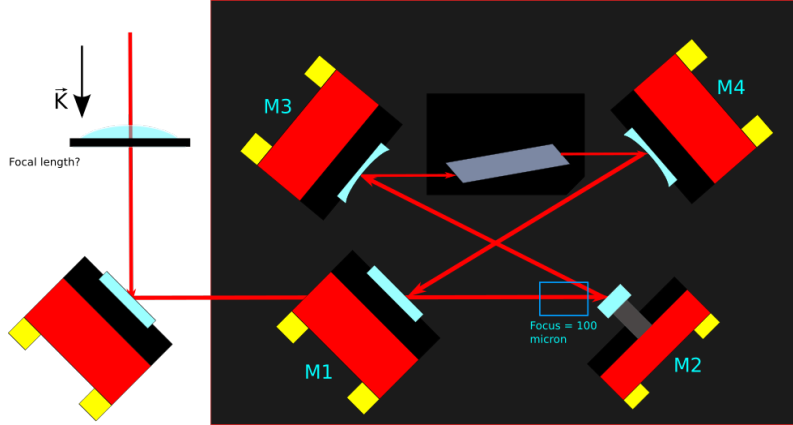


Figure 17: *Schematic illustration of the enhancement cavity. The incident light is coming from the bottom left corner and is transmitted through a partly reflecting mirror to couple the light into the cavity. The blue lined square is where the small focus with a $100\mu\text{m}$ waist must be located.*

Before starting trying different lenses, one can observe the current situation where collimated light is emitted from the fiber with a waist around $400 \mu\text{m}$, as shown in figure 16. The focus must have a $100 \mu\text{m}$ waist. The waist can be bigger or smaller than $100 \mu\text{m}$, but this results in less efficient coupling.

The fiber transmits only the fundamental mode, which makes it possible to use Gaussian optics, which simplifies calculations and assumptions. To determine the focal length of the lens that is required, one can state that this depends on the waist size before the lens and on the wavelength of the light. Equation 4 describes the waist size assuming Gaussian optics. Equation taken from [5]:

$$\omega_2 = \frac{2f\lambda}{\pi(2\omega_1)} \quad (4)$$

Where ω_2 is the waist size of the focal spot after the lens, f is the focal length of the lens, λ is the wavelength of the light and ω_1 is the waist size of the incident light. Consequently, rewriting equation 4 to a form where f is the sought-after parameter:

$$f = \frac{\pi\omega_2\omega_1}{\lambda} \quad (5)$$

Filling equation 5 with ω_2 is $100 \mu\text{m}$, ω_1 is $400 \mu\text{m}$ and the wavelength at 626 nm , one can retrieve a focal length of 200 mm . Fortunately, this lens is available in the lab and is used to focus the light into the cavity.

4 Second Harmonic Generation to 313 nm

This chapter will describe the process of SHG and the nonlinear crystals enabling this process. SHG scales non linear with the fundamental optical power and therefore high fundamental light is desired. Therefore, a resonance cavity is build to let the fundamental light pass multiple times trough the crystal since a the single pass efficiency is very low at low fundamental power. Second harmonic generation is a process where two waves with frequency ω (fundamental light) are combined to one wave with frequency 2ω (second-harmonic light). Finally, the power buildup of 626 nm light in the resonance cavity will be adressed as this is a result of the cavity characteristics.

Ideally, all the 626 nm light is trapped inside the cavity. Therefore, entering the cavity is not allowed either. Effective incoupling can be achieved by destructively interfere the reflected light from the incoupling mirror with transmitted light from the cavity. The reflected light does not get phase shift of 180 degrees (π) since the surface of the mirror has a higher refractive index than air. The transmitted light does get a phase shift, because the transmitted light does experience the 3 mirrors, each accountable for a π phase-shift. When the transmitted light meets the resonance condition ($\delta = 2m\pi$) after a cavity round trip, part of the light gets transmitted from inside the cavity by the incoupling mirror. The phase difference between the reflected light and the light coming from the cavity is exactly π , resulting in destructive interference and therefore no light can be observed reflecting at the incoupling mirror. The situation is depicted in figure 18

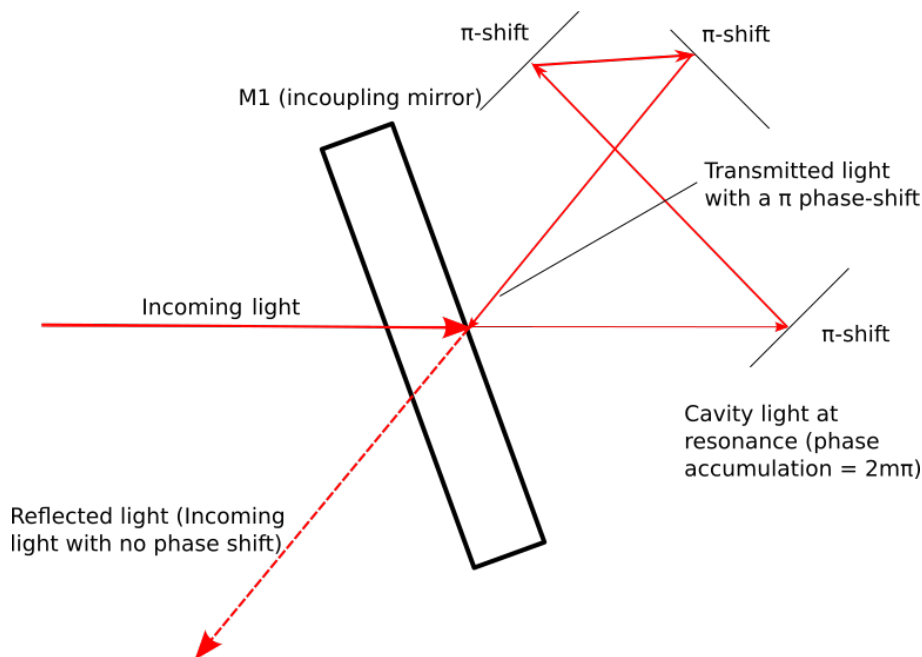


Figure 18: *The schematic shows the condition of effectively coupling light to the cavity. The roundtrip phase accumulation has to be exactly $2m\pi$ to destructively interfere with the reflected light, resulting in efficient light incoupling.*

4.1 Hänsch-Couillaud

In order to build up power, the cavity must be in resonance with the frequency of the laser light. Due to external disturbances such as temperature fluctuations, acoustical disturbances, and electrical noise, both the frequency of the laser light and the resonance frequency of the cavity are continuously changing. As a result, a stabilization strategy is applied in the cavity that actively alters the cavity's path length by having one mirror on a piezo (PC4FL from Thorlabs), keeping the cavity in resonance with the laser light's

frequency. The stabilization system deduces a feedback signal from the leftover reflected light from the incoupling mirror using a technique developed by Hansch and Couillaud [8]. The approach examines the reflected beam's polarization state and extracts the cavity's length mismatch.

A polarized laser beam is coupled into the cavity, which contains a linear polarizer positioned at an angle θ to the polarization axis of the beam. The polarization component of the beam that is orthogonal to the intracavity polarizer suffers significant losses and hence does not pass into the cavity. As a result, the incoupling mirror (mirror M1 in figure 19) will reflect this polarization component. The polarization component of the beam parallel to the intracavity polarizer suffers no losses, allowing it to perform a roundtrip to interfere with the incoming beam at the incoupling mirror M1 and therefore achieve effective beam incoupling.

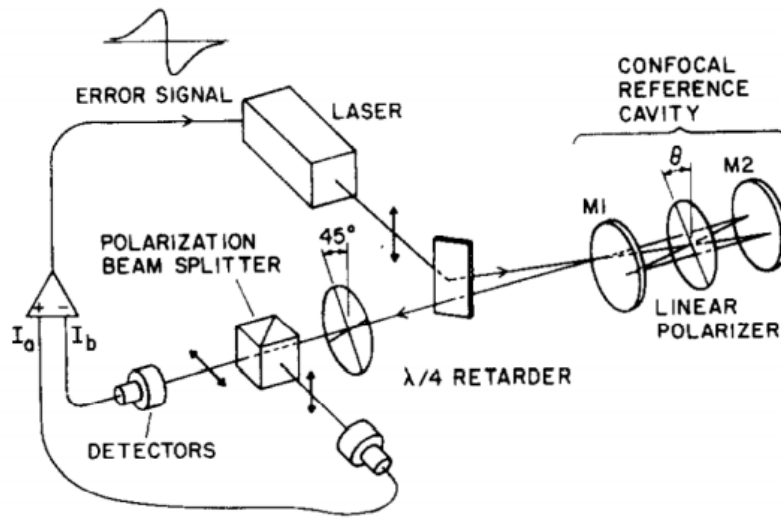


Figure 19: Hänsch-Couillaud locking scheme. The laser contains a cavity which in our setup is the resonance cavity. The error signal produced by a phase-difference due to the cavity length mismatch is sent to a PID controller in this cavity. This error then gets amplified with a high-voltage amplifier and is then sent to

The amount of reflected light from mirror M1 is determined by the cavity's travel length and hence by the interference. The two reflected polarization components from mirror M1 have now combined to generate an elliptical polarization, with the amount of ellipticity determined by the cavity path length. The quantity of ellipticity is conveyed in the amplitudes of these circularly polarized components because elliptical polarization is a superposition of left-handed and right-handed circularly polarized components with distinct amplitudes. A quarter-wave plate and a polarizing beamsplitter cube are used to split the two circularly polarized components in order to measure their amplitude. The fast axis of a quarter-wave plate is angled 45 degrees relative to the transmission polarisation of a beamsplitter cube. The two circular polarized components will be separated as a result, and their amplitude may be detected successfully with a photodiode. The differential intensity is measured using two photodiodes (FDS100-P5) in a balanced photodiode configuration. According to [8], the resulting error signal is:

$$I_{diff} = 2I_0 \cos(\theta) \sin(\theta) \frac{T_{in} R_{in} \sin(\delta)}{4(1 - R_{in})^2 R_{in} \sin(\frac{1}{2}\delta)^2} \quad (6)$$

where I_0 is the incoming laser beam intensity, T_{in} and R_{in} are the incoupling cavity

mirror's transmissivity and reflectivity, and δ is the phase difference between the electric fields in successive cavity round-trips. The phase mismatch is either positive or negative, depending on how much the cavity length is off from the laser frequency, and it affects which way the path length should be modified to keep the cavity in resonance.

To achieve maximal incoupling effectiveness, the angle between the polarisation of the incoming light and the polarizer (θ) must be near 0 degrees, but in reality, a small amount of reflected polarisation is sufficient to record a difference signal. Typically, the error signal is sent into a PID controller to create a feedback signal, which is amplified in a high-voltage amplifier to drive the piezo with an appropriate bandwidth.

Figure 20 shows the error signal that is produced by measuring the reflected light while letting the piezo element scan the cavity length. The reflected light is made from linear to circular using a $\frac{\lambda}{4}$ waveplate and is split up in two components with a polarising beamsplitter cube and the two light components are measured independently using two different photo-diodes. The current that is created by the photo-diodes can be summed up. If there is equal amount of light shone on both photo-diodes, the sum of the current made by the photo-diodes equals zero. When more light of one polarisation is shone onto one of the photo-diodes, the sum of current from both photo-diodes does not equal zero and consequently a difference in voltage can be measured.



Figure 20: *Reflection of the incoupling mirror while the piezo is scanning the cavity length. When the cavity is close to resonance, the difference in phase is measured due to different polarised light. The cavity is resonant when the round trip phase accumulation is equal to $2m\pi$ and only reflected polarisation is measured. The difference in current between the two photodiodes becomes 0 and therefore the voltage goes to 0. This signal is used to feedback a PID controller connected to the piezo, keeping the cavity in resonance.*

4.2 Phase matching in nonlinear crystals

”Phase matching” implies for type I phase matching that the sum of the two fundamental k-vectors is equal to the k-vector of the frequency-doubled light (Equation 7). These k-vectors are defined by the indices seen by each one of the beams. These indices are for the fundamental the BBO ordinary index at 626 nm (doesn't depend on angle), and for the frequency-doubled light an index set by the phase matching angle which sets the relative contribution of the ordinary and extraordinary indices.

$$\Delta k = k_{\text{harmonic}} - 2k_{\text{fundamental}} \quad (7)$$

After crossing a given distance within the crystal, the harmonic light will be destructively interfered due to a $\pi/2$ phase mismatch with the fundamental light, which can be as

little as 10 μm for a commonly used crystal like BBO. A specific configuration needs be found where $\eta^\omega = \eta^{2\omega}$ ($\eta_e^{2\omega}(\theta_m) = \eta_o^\omega$ for negative birefringent crystals and $\eta_e^\omega(\theta_m) = \eta_o^{2\omega}$ for positive birefringent crystals) in order to leverage extended interaction lengths. The symbol η represents the refractive index specified by the light frequency ω . The angle θ_m is the phasematching angle and is defined as the angle between the propagation of the light and the optical axis. The definition of negative or positive crystals is defined as:

$$\Delta\eta = \eta_e - \eta_o \quad (8)$$

For negative birefringent crystals, the ordinary refractive index is greater than the extraordinary refractive index and therefore the sum is smaller than zero. In addition, for positive birefringent crystals the sum is greater than zero.

A birefringent crystal can be used to match the refractive indices of different wavelengths by polarizing the fundamental and harmonic waves differentially with respect to the optical axis (ordinary (o) waves for perpendicular polarization and extraordinary (e) waves for parallel polarization). The type of phase matching used in this arrangement is type-I. The fundamental polarisation (o polarisation) is orthogonal to the harmonic polarisation (e polarisation) in type-I phasematching .

The refractive index of the e-wave can be changed by rotating the optical axis between the direction of extraordinary polarization and the beam propagation direction. Figure 21 shows a schematic of the refractive indices (y-axis) as function of the light frequency (x-axis). One can see that the fundamental frequency ω is the ordinary polarisation and the harmonic frequency 2ω is the extraordinary polarisation. This scheme is for a negative uniaxial crystal like BBO, since the refractive index for the ordinary polarisation is greater than the refractive index for the extraordinary polarisation.

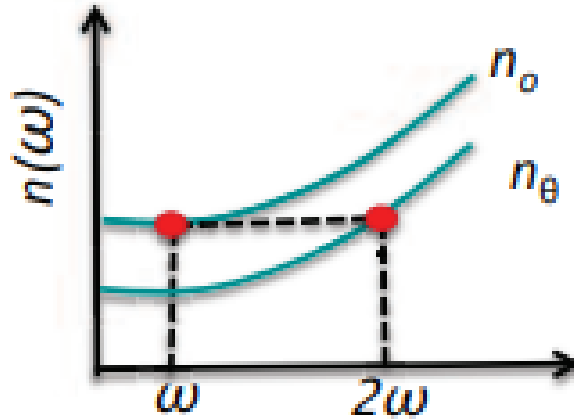


Figure 21: A schematic of the refractive index (n) as function of frequency (ω). This image represents a negative birefringent crystal since the ordinary refractive index is greater than the extraordinary refractive index. The crystal can be oriented such that the refractive indices match for both ordinary as extraordinary polarisation. Taken from [9]

Figure 22 displays the orientation of the optical axis with respect to the light propagation vector \vec{k} to match the refractive indices. This image is taken from [7].

Because the refractive index surfaces are wavelength-dependent, various phasematching angles θ_m will be discovered for different wavelengths. Angle-tuning is the process of matching phase by adjusting the angle. The optical axis angle θ_m determines the refractive index of the e-wave, which is given by:

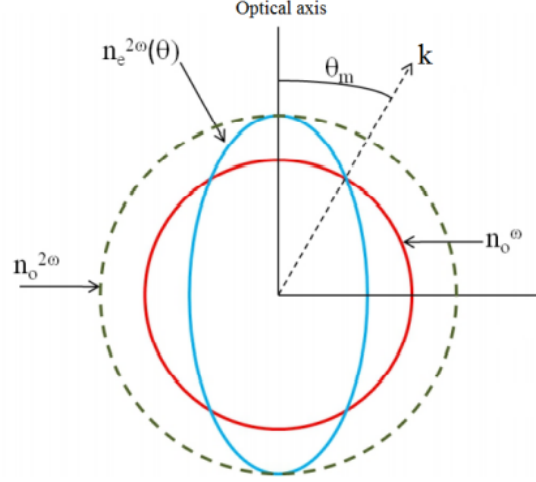


Figure 22: This image represents a negative birefringent crystal. Negative means that the refractive index for ordinary waves is greater than the refractive index for extraordinary waves. The ordinary-wave with frequency ω and the extraordinary-wave with frequency 2ω have refractive index surfaces where θ_m is the angle between the wave vector \vec{k} and the optical axis at which the two refractive indices meet. Taken from [7]

$$\eta_e^{2\omega}(\theta_m) = \frac{\eta_e^{2\omega} \eta_o^{2\omega}}{\sqrt{(\eta_o^{2\omega})^2 \sin^2 \theta_m + (\eta_e^{2\omega})^2 \cos^2 \theta_m}} \quad (9)$$

The phasematching angle can be obtained by applying the constraint $\eta_e^{2\omega}(\theta_m) = \eta_o^\omega$ and the identity $\cos^2 \theta_m = 1 - \sin^2 \theta_m$ to equation 9. Taken from [7]:

$$\theta_m = \sin^{-1} \left(\sqrt{\frac{(\eta_o^\omega)^{-2} - (\eta_o^{2\omega})^{-2}}{(\eta_e^{2\omega})^{-2} - (\eta_o^{2\omega})^{-2}}} \right) \quad (10)$$

Using equation 10 for BBO and LBO gives $\theta_m = 38.4^\circ$ for BBO and $\theta_m = 90^\circ$ for LBO.

4.2.1 Intracavity polarizer

The crystal is used as a polarization-selective element in the cavity for the Hansch-Couillaud locking scheme. By using a crystal cut at Brewster angle for the fundamental light, the transmittance through the crystal can be maximised and more power can buildup in the cavity. Brewster angles for BBO and LBO are 59.05° and 58.26° respectively at 626 nm. Also, the s-polarisation with respect to the Brewster gets reflected on the incoupling mirror and can be used for the Hansch-Couillaud locking scheme. However, the downside on using a Brewster for the fundamental waves is that the harmonic polarisation is orthogonal to the fundamental polarisation and therefore around 16% of the harmonic light gets reflected on the back-end of the crystal. Figure 23 shows the reflectivity as function of angle of incidence for both s- and p-polarization. As the p-polarization gets closer to the Brewster, the s-polarization gets more reflected. Each wavelength has a different Brewster angle since the refractive index is wavelength dependent.

The quality of the Brewster cut for the BBO crystal is measured using p-polarized light emitted on to the Brewster surface and observing what the reflected optical power is versus the initial optical power. The polarization beamsplitter only allows p-polarisation to

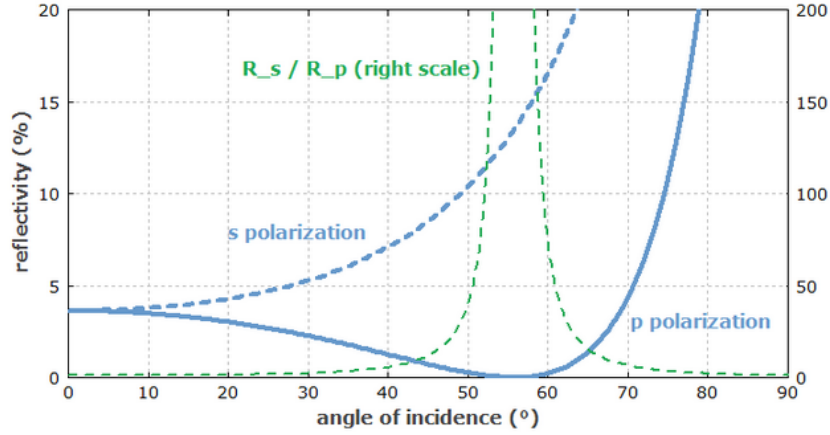


Figure 23: The reflectivity as function of angle of incidence for s- and p-polarization. The p-polarization is fully transmitted at Brewster while the S-polarization is between 12 and 16 % reflected. The amount of reflection is per surface. This specific image is for a air/silica interface at 1064 nm. Taken from [10]

pass through, this determines the polarisation shone on the crystal by rotating the polarization beamsplitter cube. The p-polarisation for the Brewster is set by matching the p-polarisation from the cube to the crystal. Figure 24 shows the setup for this measurement. A $\frac{\lambda}{2}$ waveplate for a range from 400 to 800 nm (AHWP10M-600) is used to set the orientation of the linear polarised light. The polarisation was set by measuring the maximum transmission or reflection at the second beamsplittercube.

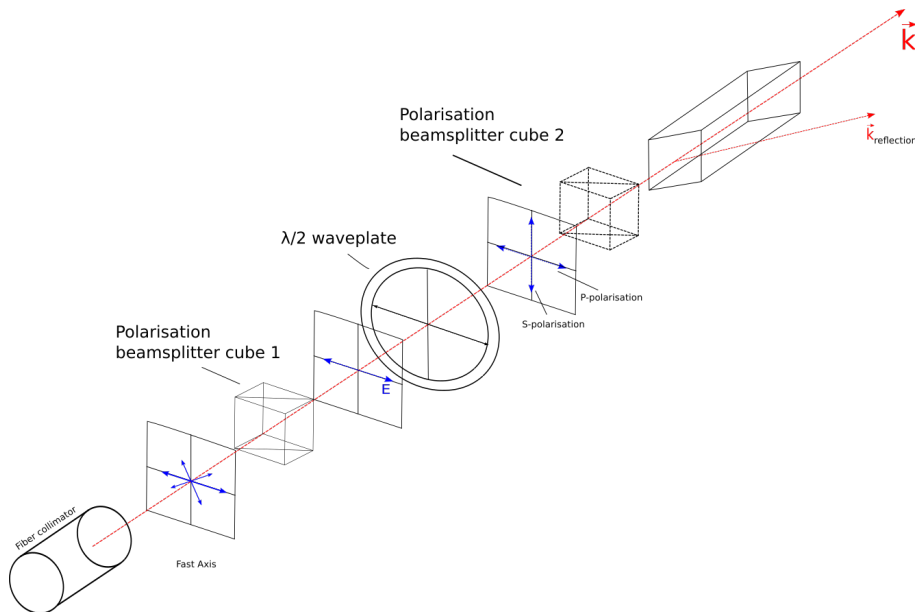


Figure 24: The setup for measuring the quality of the crystal Brewstercut. Linear polarized light can be oriented with the $\frac{\lambda}{2}$ to match the p- or s-polarization of the beamsplittercube. Beamsplitter cube 2 was removed for measuring the transmission and reflection for s-polarisation. The orientation of the polarisation can be set by rotating the $\frac{\lambda}{2}$ -waveplate.

The initial quantity of optical power before the beamsplitter cube is 1.77 ± 0.02 mW and the reflected power is 3.6 ± 0.4 μ W. This gives a reflection percentage of around $2 \cdot 10^{-3}$ %, which is close to zero. This complies with the expectations for reflection at p-polarisation with respect to the Brewster. Additionally, one can look at the transmission of p-polarized light, which is expected to be close to 100%. The transmission is 1.95 mW with respect to the 2.05 mW of initial optical power, which gives a transmission percentage of around

95 %. The transmission is not 100 % because the light is scattered inside the crystal.

Previous measurement used p-polarised light with respect to the Brewstercut. The same measurement for reflection and transmission can be executed for s-polarised light. Figure 23 shows that the reflection for s-polarised light is around 16% per surface at Brewsterangle.

The crystal has two surfaces which are at Brewster, so the expected transmission depends on the reflection on both Brewster surfaces. The reflection on one Brewster surface for s-polarised light is around 16% so the transmission is 84% of the light. The total transmission can be expressed as $T_{\text{surface1}} \cdot T_{\text{surface2}}$, $0.84 \cdot 0.84 = 0.70$, so around 70% transmission is expected for s-polarised light. The initial power is 2.02 ± 0.02 mW and the transmitted light is 1.325 ± 0.02 mW. This transmission is 65.5%, so close to 70%. The uncertainties are taken into account, but these are not important since the measurement is only a relative measurement. From these measurements, one can conclude that the BBO has a proper cut at Brewster. All measurements are included in table 1.

Table 1: *The transmission and reflection percentages for s- and p-polarisation for a BBO-crystal cut at Brewster angle.*

BBO	Theoretical	Measured
Reflection 1 st surface, p-polarisation	0%	$2.0 \cdot 10^{-3}\%$
Reflection 1 st surface, s-polarisation	16 %	15%
Transmission, p-polarisation	100%	95%
Transmission, s-polarisation	70%	65.5%

4.3 Crystal axis

The phasematching angle and the Brewster angle for both the BBO and the LBO crystal are known. With this, one can compute the orientation of the optical axis in the crystals. First, BBO will be computed as this is an uni-axial negative birefringent crystal which makes computation easier. Figure 25 shows the theoretical expectation of the configuration. Ordinary refractive index is experienced by fundamental light, hence this fundamental polarisation must be orthogonal to the optical axis in order to experience ordinary refractive index.

The fundamental light has to be refracted in the vertical (y-direction) according to the refractive indices which are polarisation dependent. One can check the orientation of the optical axis of an uniaxial birefringent crystal by shining a collimated beam into the crystal and look at the transmitted beam. The polarisation of the collimated can be both linear as well as circular, as long as the light contains p- and s-polarised light. One can observe that refraction is horizontal with the BBO crystal in the lab. This means that the optical axis is rotated with 90 degrees around the z-axis as shown in figure 26. As a result, phase matching cannot be achieved by sending p-polarised light into the crystal. As a consequence, the crystal cannot be used inside the resonance cavity.

Another possibility is using a LBO crystal for phasematching. A LBO crystal is biaxial, which means that the crystal has 2 optical axis. The optical axis in a biaxial crystal has angle ϕ ($\phi = 56.3^\circ$) for LBO at 626 nm) with x-axis. The phase-matching angle, the angle between the light propagation vector \vec{k} and the optical axis for meeting refractive indices, is 90° for LBO at 626 nm.

Because of the two optical axes in the crystal, checking an LBO crystal is difficult. As a result, a check is done in the lab using a new set-up in which orders of magnitude of hundreds of milliWatts can be aimed directly at the BBO crystal to examine if 313 nm

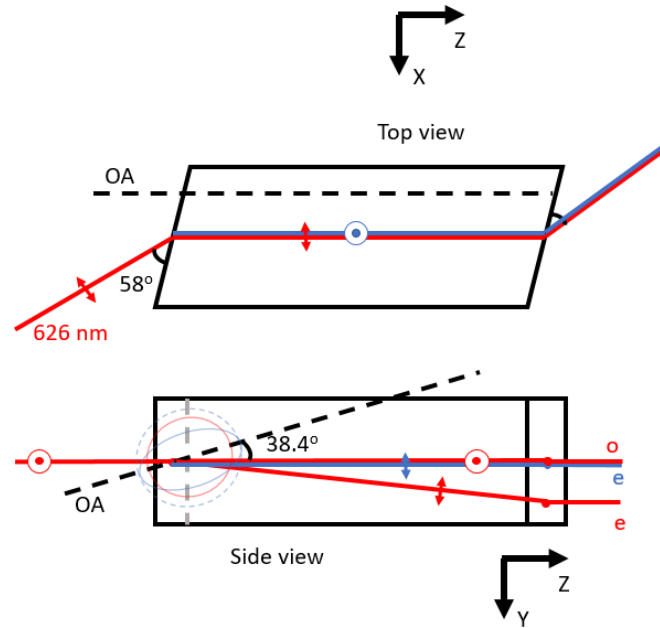


Figure 25: *The expected configuration for the BBO crystal. The optical axis is oriented so that ordinary polarised light experiences the ordinary refractive index. The propagation of light has an $\theta_m = 38.4^\circ$ with respect to the optical axis. Image taken from [11].*

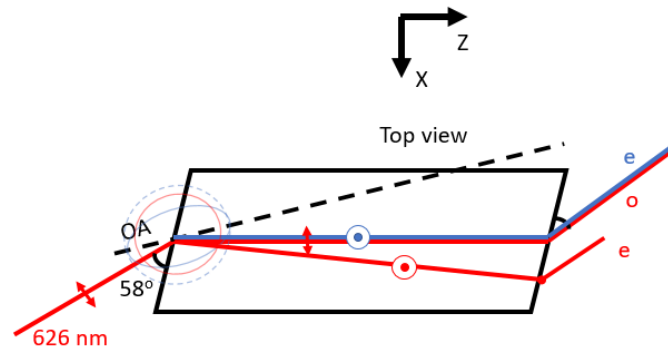


Figure 26: *Measured refraction of fundamental light inside the crystal. The optical axis is rotated with 90 degrees around the z-axis, which mean that phasematching cannot be achieved for fundamental p-polarised light. Image taken from [11]*

light can be created. To boost the intensity of the light, a lens is employed to focus it on the crystal, but no 313 nm was observed.

According to F.M.J Cozijn, conversion efficiency for a BBO- and LBO crystal are 1.91 pm/V and 0.51 pm/V respectively. The conversion efficiency is 3 to 4 times higher for BBO then for LBO. Therefore, this setup will use the BBO crystal. However, the LBO has less beam walk-off for 313 nm then BBO, so for setups where high fundamental power can be delivered (1 Watt) LBO is preferred. All properties for both BBO- and LBO crystals are displayed in 2

Table 2: *The properties of nonlinear crystals BBO and LBO. Table taken from [7].*

Property	BBO	LBO
Crystal class	negative uniaxial	negative biaxial
Phase matching type	type 1	type 1
n_o^ω	1.667	1.616
Brewster's angle	59.05°	58.26°
θ_m	38.4°	90°
ϕ	0°	56.3°
Walkoff-angle	80.37 mrad	17.60 mrad
NLO coefficient	1.91 pm/V	0.51 pm/V

4.4 Characteristics of the cavity

The resonance cavity is used to build up optical power for 626 nm light which is used for generating 313 nm light. The amount of optical power build up and the conversion efficiency depends on the characteristics of the cavity such as the cavity finesse, Q-factor, Full Width Half Maximum (FWHM), Free Spectral Range (FSR) and the light incoupling efficiency. This paragraph describes the theoretical and measured characteristics of the resonance cavity designed by F.M.J. Cozijn. [7].

4.4.1 Finesse

A property of a resonance cavity is the finesse. The finesse states the frequency difference between two resonant frequencies. For a resonance cavity, the finesse depends on the cavity losses and therefore on the reflectivity of the mirrors. High reflective mirrors have less losses and therefore a cavity obtains a higher finesse. The finesse relates to the optical power buildup in a cavity, because less losses means higher power buildups.

The purpose of the resonance cavity is to enhance the optical power in 626 nm. Therefore, high reflective mirrors (99.998%) for 626 nm are used. Only the incoupling mirror (M1 in figure ..) has a reflectivity of 98.8%. The optical power losses mainly depend on the leakage through the incoupling mirror. The optical power losses also depend on the reflection on the intracavity polarizer and the conversion efficiency.

Figure 27 shows the reflection dips (yellow line) from the incoupling mirror while the piezo mirror is scanning the cavity length (orange line). The piezo extends as the voltage increases across the piezo (orange line with positive slope), shortening the cavity length. The voltage increment is linear, so the cavity decreases linear in length. However, the frequency ramp is not linear since the difference in resonant frequencies (Free spectral range) depends on $\frac{n \cdot c}{L + \Delta L}$.

Looking at the width of reflection dips does not state the FWHM, because when the slope of voltage increment increases in steepness, the width of the dips decreases. The same applies to the distance between two transmission dips. However, the ratio between the width of a transmission dip and the distances between two transmission dips remains the same. This is defined as the finesse. The finesse is measured with the crystal in the cavity, otherwise the cavity cannot be closed and as a result no successive cavity round trips can take place.

The width of a peak halfway its maximum is 0.015 ± 0.003 ms as the distance between two transmission dips is 5.7 ± 0.2 ms. This gives a measured finesse of 380 ± 78 ¹.

4.4.2 The free spectral range of the resonance cavity

The separation of an optical resonator's axial (Gaussian-shaped) resonator modes in terms of optical frequency is its free spectral range. Formula 11 gives the FSR for a bow-tie cavity. A factor 2 is implemented for a two-mirror cavity, but the factor 2 can be removed because the bow-tie cavity is a single-pass cavity.

¹ $\Delta Finesse = \sqrt{\left(\frac{\delta A}{A}\right)^2 + \left(\frac{\delta B}{B}\right)^2} \cdot \frac{A}{B}$

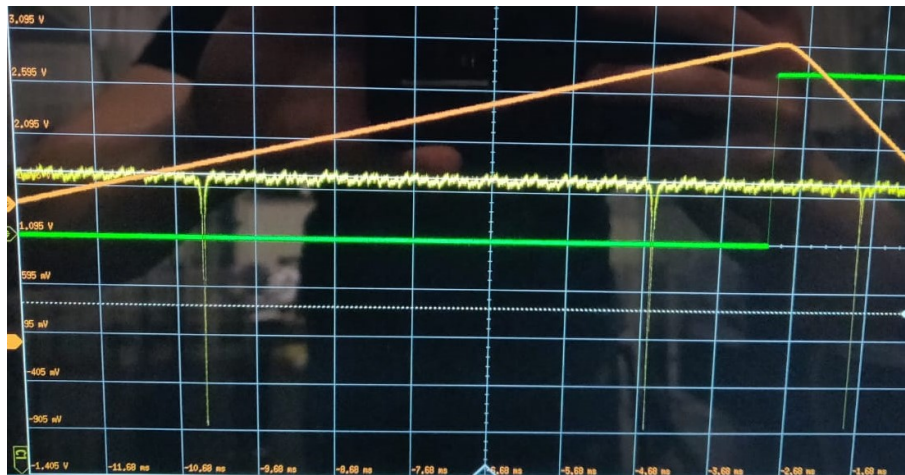


Figure 27: Measurement of the finesse. The orange line is the voltage applied onto the piezo, decreasing the cavity length. The yellow line represents the reflection of the 626 nm light on the incoupling mirror. The cavity length is running and at resonance for 626 nm light, the light gets coupled in and there is less reflection (dips in yellow line). The green line is a trigger of the piezo voltage ramp.

$$\delta_{FSR} = \frac{c}{L} \quad (11)$$

Where δ_{FSR} is in Hertz (s^{-1}), c is the speed of light ($299\,792\,458\text{ m s}^{-1}$) and L is the cavity length ($26.4 \pm 0.5\text{ cm}$). Filling this in for equation 11 gives an FSR of $1.136 \cdot 10^9 \pm 0.008 \cdot 10^9\text{ Hz}$ or $1.136 \pm 0.008\text{ GHz}$ for a fixed cavity length at 26.4 cm . However, the free spectral range changes with changing cavity length. The change in cavity length is to go from resonance mode M to $M+1$ is one wavelength at 626 nm . The change in cavity length is sufficiently small with respect to the cavity length that the change in free spectral range can assumed to be linear.

4.4.3 The full width half maximum of the resonance cavity

The FWHM is a result of the finesse of the cavity. The finesse was previously described as the ratio between the FWHM and the FSR. The finesse and the FSR are known and can be used to determine the FWHM for this cavity. The equation for determining the FWHM is given by:

$$FWHM = \frac{\delta_{FSR}}{Finesse} \quad (12)$$

Using this equation with the $\delta_{FSR} = 1.136 \pm 0.008\text{ GHz}$ and the finesse at 380 ± 78 , the $FWHM = 2.98\text{ MHz} \pm 0.61\text{ MHz}$.

4.4.4 Q-factor

The Q-factor for an optical resonator states how quickly the energy gets dissipated from the resonator. A high Q-factor states that the time to dissipate the energy from the resonator takes relatively long and higher optical power buildups can take place.

The Q-factor can be described in multiple ways for an optical resonator. One description is the Q factor is the ratio of the resonance frequency ν_0 and the full width at half-maximum (FWHM) bandwidth $\delta\nu$ of the resonance (equation 13) [12].

$$Q = \frac{\nu_0}{\delta\nu} \quad (13)$$

With ν_0 is the frequency of the 626 nm light (4.79 THz) and $\delta\nu$ is $2.98 \pm 0.61\text{ MHz}$, Q-factor is $1.6 \cdot 10^8$. Additionally, The Q-factor depends on the optical frequency ν_0 , the fractional power loss per roundtrip l and the roundtrip time τ_{rt} according to [12] and be described as equation 14

$$Q = \frac{2\pi\nu_0\tau_{rt}}{l} \quad (14)$$

The roundtrip time can be described as the cavity length ($26.4 \pm 0.5\text{ cm}$) divided by the speed of light, so the roundtrip time is $0.88 \pm 0.02\text{ ns}$. The roundtrip loss is estimated to be around 1.2% , because the incoupling mirror is only reflecting for 98.8% and assuming that there are no losses caused by the intracavity polarizer. Filling in the equation gives an Q-factor of $2.2 \cdot 10^8$. The discrepancy between the two values for the Q-factor can possibly explained the losses caused by the intracavity, which are not taken into account with the second calculation.

4.4.5 The power enhancement by the resonance cavity

The power build up of the fundamental light within the cavity must be understood in order to determine the quantity of second harmonic power produced by the crystal. Due to a resonance condition of the cavity, which causes a power accumulation of the incoming light onto the cavity, the fundamental light in the cavity is boosted. The enhancement factor is calculated using the cavity's round-trip losses. The reflection losses of mirror coatings and crystal surfaces, the conversion losses within the crystal, and the residual absorption and scattering of the fundamental light inside the crystal all contribute to these losses. An incoupling mirror with a transmission close to the cavity round-trip losses is utilized to compensate for these losses. The reflected light will be suppressed due to destructive interferences, effectively coupling light into the cavity which is similar to impedance matching. The incoupling efficiency for this setup is around 90%, but it can be optimized till 95%. The 90% incoupling efficiency is a result of beam shaping, setup alignment and mode cleaning. The intracavity power is derived by F.M.J Cozijn [7] and is given in the following equation:

$$P_{cav} = P_{on} \frac{T_i}{(1 - \sqrt{R_c R_i})^2} \quad (15)$$

Where P_{cav} is the intracavity power, P_{on} is the incoming power on the cavity incoupling mirror, T_i is the transmission trough the incoupling mirror, R_c is the cavity's reflectivity and R_i is the reflectivity of the incoupling mirror. From this relationship it can be deduced that when $R_i = R_c$, optimum impedance matching is achieved and therefore the enhancement factor (P_{cav}/P_{on}) is maximized. The intracavity power then becomes:

$$P_{cav} = \frac{P_{on}}{1 - R_c} \quad (16)$$

It's worth noting that all incident light on the cavity will be coupled into the cavity on resonance. Equation 16 can be used to compute the cavity round-trip power for different cavity parameters and then determine the actual value of R_c ($=R_i$) and the actual dependence of a tiny impedance mismatch because R_c can be chosen. For this project, a 98.8% reflectivity for the incoupling mirror is chosen. The roundtrip losses are composed of the finite reflection of the remaining mirrors (R), transmission through the crystal (T_c), and loss due to harmonic conversion in the crystal (T_{SH}), with $T_{SH} = 1 - P_{cav}^2 \gamma$. γ is the conversion efficiency of a non linear crystal with specific length. The comparable reflectivity of a bow-tie cavity, R_c , with three reflective mirrors in addition to the incoupler is:

$$R_c = R^3 T_c T_{SH} \quad (17)$$

T_{SH} is a power-dependent loss, which means that at greater power levels, the comparable reflectivity will be reduced. At low roundtrip power ($T_{SH} \ll T_c$) the transmission losses through the crystal are the primary loss factor, since the mirror reflectivities are often close to 100%. Depending on the crystal composition and surface reflection losses, transmission losses through a crystal range from 0.5 to 2% [7]. The Brewster angle maximizes transmission as discussed in section 4.2.1. Figure 28 shows the influence of the incoupler's reflection value on impedance for various loss factors. The red vertical line in figure 28 shows the chosen reflectivity for the incoupling mirror (0.988). The enhancement depends on the reflectivity of the incoupling mirror, but also on the intracavity losses. Therefore, three lines are plotted representing various values for intracavity losses. The power enhancement is between 60 and 120 times the incoupling power for a 98.8% reflectivity when the losses are between 0.8 and 1.5%.

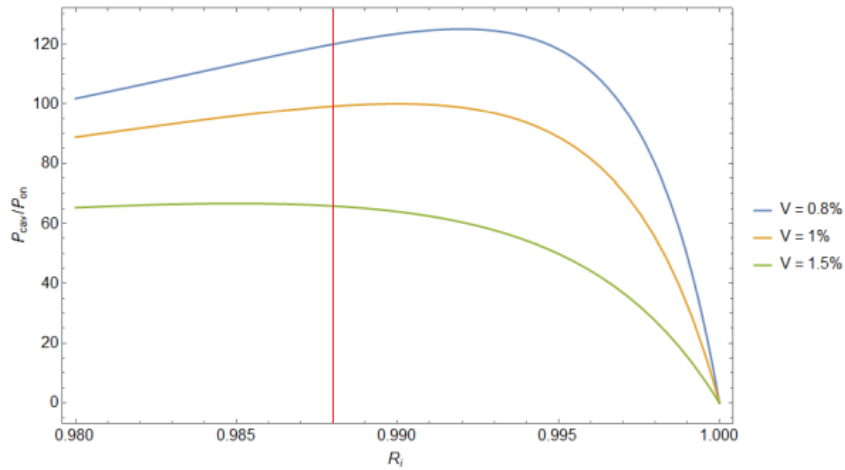


Figure 28: Power enhancement as function of the incoupling mirror reflectivity. The three curved lines are the power enhancement as function of reflectivity for various intracavity losses. The red vertical line is the selected reflectivity for the incoupling mirror (0.988). Image taken from [7]

As described in chapter 2, the optical power that can be delivered at 626.266 nm is around 15 mW after the optical isolation. The transmission through the fiber is 56%, which means that only around 8 mW can be used for cavity incoupling. The incoupling efficiency is 90% for this setup, this means 7 mW is injected into the cavity for enhancement. As a result, the intracavity power becomes between 60 and 120 larger and therefore the intracavity power is between 420 and 840 mW. Note that this is only with perfect mode-matching and without any frequency noise.

5 The characterisation of 313 nm light

Previous chapter described the resonance cavity used for obtaining more optical power at 626 nm for conversion to 313 nm. This chapter describes the theoretical and measured optical power at 313 nm. However, the BBO crystals were not manufactured as expected, resulting in a BBO crystal in which the phase matching condition cannot be fulfilled for p-polarised light. Consequently, the crystal cannot be used inside the resonance cavity for SHG. Therefore, only theoretical predictions can be made on based on the calculations and assumptions given by [7].

5.1 Optical power at 313 nm

The intracavity power of 626 nm affects the conversion to 313 nm. Together with the intracavity power, the length of the crystal also affects the conversion from 626 to 313 nm. Figure 29 shows the conversion coefficient (γ) as a function of crystal length (l) for both BBO and LBO crystals. The red vertical line in this figure is selected length of 12 mm for the crystals. The crystal length of 12 mm is set as optimum, because crystals longer than 12 mm do not drastically increase the conversion efficiency. In addition, the resonance cavity designed by F.M.J. Cozijn had to remain as small as possible to avoid wasting space, which is important for setups where not much space is available.

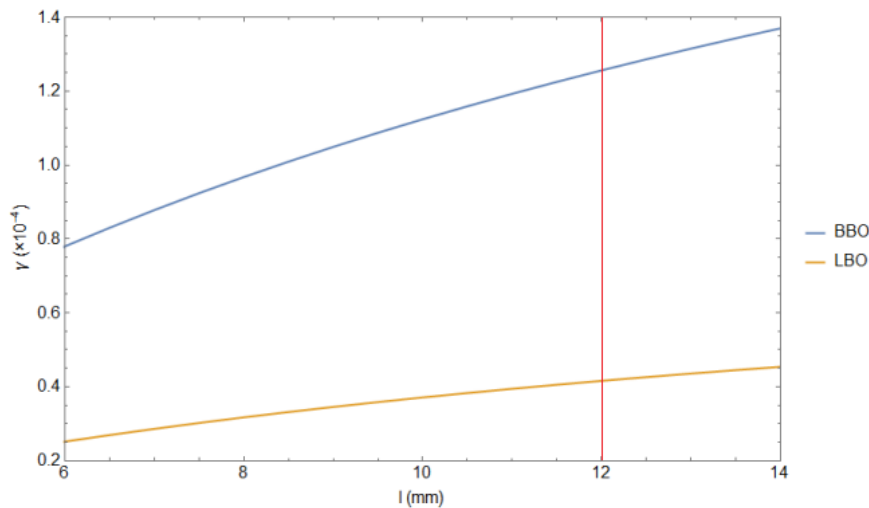


Figure 29: The conversion efficiency of BBO- and LBO crystals as function of different crystal lengths. The length for both crystals is 12 mm (red vertical line) Image taken from [7]

The conversion coefficient γ for BBO is around $1.3 \cdot 10^{-4}$ and for LBO this is around $0.4 \cdot 10^{-4}$ for a crystal length of 12 mm. This means that BBO is 3 times more efficient at converting 626 nm light to 313 nm light. The intracavity power is known as function of the incoming light onto the cavity and the reflectivity of the incoupling mirror. The conversion coefficient is known as function of the crystal length. Equation 18 gives the optical power for the harmonic light as function of the intracavity power and the conversion coefficient. This equation can be used to give an expectation of the amount of harmonic light.

$$P_{har} = P_{on}^2 \gamma \quad (18)$$

One can use equation 18 to give an estimation on the harmonic power. However, equation 18 does not account for any losses in the crystal. Since the harmonic polarisation is sheer to the Brewster surface, one can state that 16% of the harmonic light is lost due to reflection. Additionally, another 5% of harmonic light is lost to reflection due to the coating on the

crystal which is anti reflective for 626 nm light. The specifications for the coating are not known and therefore assumed to only be anti-reflective for 626 nm as stated in [7]. These losses add up and the harmonic power that can be measured can be described as $P_{\text{har,measured}} = 0.8 \cdot P_{\text{har}}$. Next to that, In addition, the incident power (P_{on}) is expected to be mode matched and resonant with the cavity. In reality, there will be extra losses owing to frequency noise and inadequate mode-matching.

The measured harmonic power can be plotted as function of the incident power on the cavity for a BBO crystal. This is done by Cozijn [7] and this measurement is shown in figure 30. Notice that the harmonic power is in order of μW , but the incident power is in mW. The BBO was damaged in this measurement, which gave a total loss of 2.5% in harmonic power.

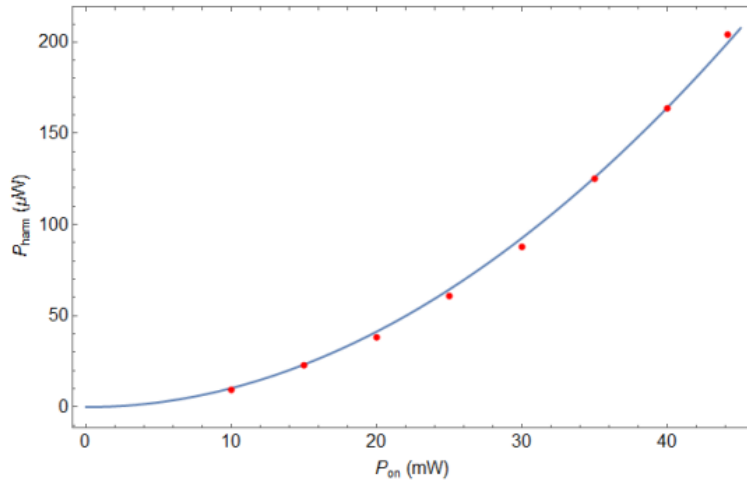


Figure 30: *Harmonic power as function of incoming power at the resonance cavity. . Image taken from [7]*

This measurement can be used to validate the estimation of harmonic power at a given intracavity power. For instance, the measurement shows using 20 mW for incident power gives around 40 μW of harmonic light. This is measured as consequence of a damaged BBO crystal. However, only around 8 mW of 626.266 nm light will be available for cavity incoupling. Therefore, harmonic power of approximately 10 μW can be measured. The intensity can be calculated to validate whether the saturation intensity of 76.5 mW/cm^2 can be reached for a beam size with a radius of 50 micron. The beam profile is estimated to be circular in shape and therefore the surface area of the beam profile is $\pi \cdot r^2$. The intensity becomes $1.27 \cdot 10^3 \text{ W}/\text{m}^2$ at a beamradius of 50 μm .

Figure 31 shows the harmonic power as function of incident power, using equation 18, with γ_{BBO} is $1.2 \cdot 10^{-4}$ and γ_{LBO} is $0.4 \cdot 10^{-4}$. This simulation is assumed to be lossless and the incoupling efficiency at 100%. Obviously, this isn't the case, but it gives a fair idea of what to expect. Note that the range of the incoupling power is closer to what the used laser diode can deliver at 626.266 nm.

However, the measured harmonic is lower because of reflections due to the polarisation with respect to the Brewster surface and the coating applied to the crystal ($P_{\text{har,measured}} = 0.8 \cdot P_{\text{har}}$), as described earlier in this chapter. The simulation of the expected measured harmonic power with correction for losses is depicted in figure 32.

The beam profile of the 313 nm is not circular, due to difference in refractive indices for p-polarised fundamental and second harmonic light. Consequently, a part of the second

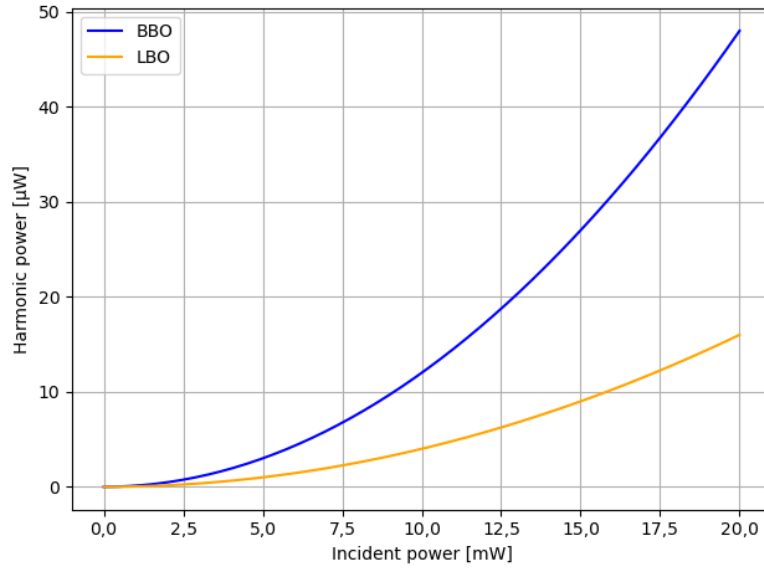


Figure 31: Simulation of the harmonic power as function of cavity incident power, assuming light incoupling efficiency is 100%. The losses in the crystal are not taken into account in this simulation.

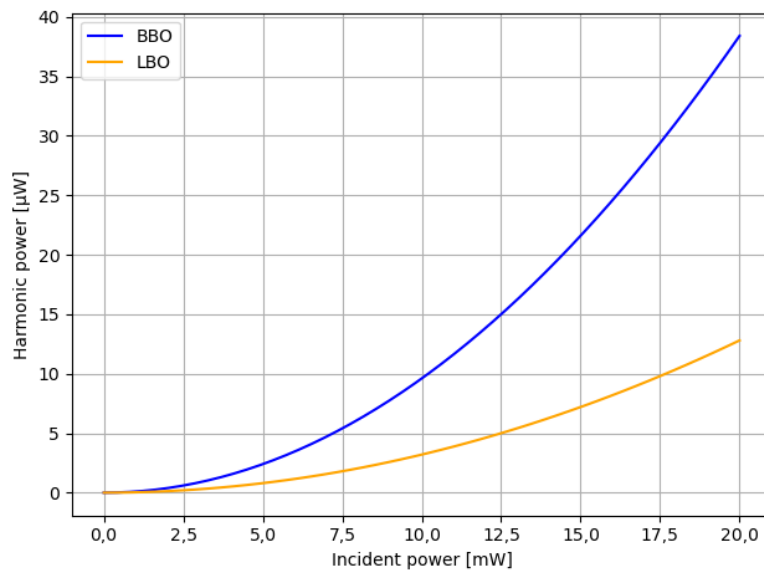


Figure 32: Assuming the incoupling efficiency is 100%

harmonic beam diverges with angle ϕ with respect to the fundamental beam. The saturation intensity is 76.5 mW/cm^2 and with that the required harmonic power as function of the beam radius of the 313 nm light (equation 19) with the saturation intensity at 76.5 mW/cm^2 can be calculated and is depicted in figure 33.

$$P_{313} = I_{sat} \cdot \pi r^2 \quad (19)$$

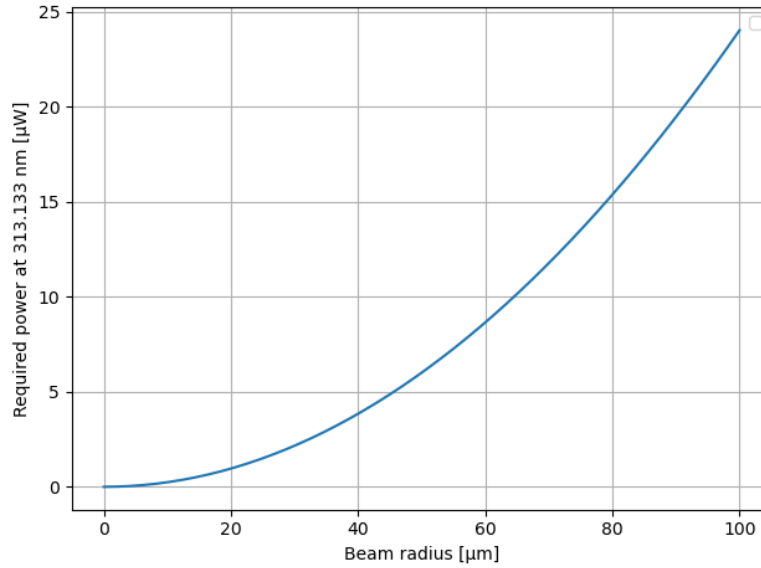


Figure 33: *The required optical power at 313 nm as function of the beam radius, assuming the beam profile is circular and symmetric. The blue line in the graph shows the bottom value for the optical power at specific radii to meet the saturation requirement of 765 W/m^2 .*

The saturation intensity is dependent on the radius of the beamprofile, together with the 313 nm power, that will be used to shine the 313 nm on the Be⁺ ions. With an incident power of around 8 mW, the measurable harmonic power becomes around 8 μW according to figure 32 and therefore a beam radius smaller than 55 μm (33) is desired to meet the saturation intensity of 76.5 mW/cm^2 . If the incident power can be increased at 626.266 nm by better fiber alignment, greater amounts of optical power at 313 nm can be achieved and therefore bigger beam radii can be used for shining Be⁺ ions. The 313 nm light needs to be coupled in to fiber, so there will optical losses.

6 Conclusion and outlook

6.1 Conclusion

The saturation intensity for the $2S_{1/2} - 2P_{1/2}$ transition in Be⁺-ions at a 313.133 nm wavelength can be achieved by enhancing 8 mW of 626.266 nm inside a bow-tie resonance cavity and frequency doubling 626.266 nm light with a Brewster-cut BBO crystal that is manufactured correctly to produce approximately 8 μ W of 313.133 nm light and then focusing the 313 nm light to a symmetric circular beam profile with a radius of less than 55 μ m. This conclusion is reached with the assumptions that there are no losses when the light is coupled into the cavity, that the loss of second harmonic light in the BBO crystal is 20% and that the power that can be coupled in does not change over time. The incoupling losses into a fiber for 313 nm are not taken into account in this calculation.

The laser diode can emit 15 mW of optical power at a wavelength of 626.266 nm. The emitted wavelength of 626.266 nm is set by the temperature inside the laser diode at 4.5 ± 0.1 °C or at a resistance of 26.17 k Ω . The beam profile emitted by the laser diode is elliptical and therefore beam shaping is required. Injection of light in single mode fiber gives the fundamental mode of the fiber, which is used to match the TEM₀₀ mode of the resonance cavity. The bow-tie resonance cavity enhances the 626 nm light between 60 and 120 times when the losses are varying between 0.8% and 1.5%. However, the second harmonic power can be calculated by the square of the incoming light multiplying with a conversion coefficient γ . This coefficient is crystal and crystal length dependent. This project makes use of BBO and LBO crystal with conversion coefficients $1.2 \cdot 10^{-4}$ and $0.4 \cdot 10^{-4}$ for a crystal length of 12 mm respectively. However, the crystals are produced with the optical axis oriented incorrectly, preventing phase-matching with p-polarised light in the resonance cavity. As a result, no 313 nm light can be produced with these crystals. The amount of 313 nm light can only be determined theoretically at this stage and not experimentally.

6.2 Outlook

The crystals were made in such a way that phase matching in the cavity was impossible. This issue has since been identified, and new crystals capable of producing 313 nm light can be ordered. Furthermore, the alignment of the single mode fiber can be improved, allowing more light to travel through the fiber and increasing the amount of light available for cavity matching. More 626 nm light will travel through the cavity, resulting in more 313 nm light being produced. As a result, the beam radius for 313 nm light can be increased, making alignment easier.

References

- [1] S. Laporta and E. Remiddi, “Quantum electrodynamics and its precision tests,” *Elsevier*, pp. 168–176, 2006.
- [2] G. Blume, O. Nedow, D. Feise, J. Pohl, and K. Paschke, “Monolithic 626 nm single-mode gainp dbr diode laser,” *Optics Express*, vol. 21, 2013.
- [3] NIST. Nist atomic spectra database lines data, be ii: 681 lines of data found z = 4, li isoelectronic sequence. [Online]. Available: https://physics.nist.gov/cgi-bin/ASD/lines1.pl?spectra=be+1&limits_type=0&low_w=&upp_w=&unit=1&submit=Retrieve+Data&de=0&format=0&line_out=0&en_unit=0&output=0&bibrefs=1&page_size=15&show_obs_wl=1&show_calc_wl=1&unc_out=1&order_out=0&max_low_energ=&show_av=2&max_upp_energ=&tsb_value=0&min_str=&A_out=0&intens_out=on&max_str=&allowed_out=1&forbid_out=1&min_accur=&min_intens=&conf_out=on&term_out=on&enrg_out=on&J_out=on
- [4] E. Optics. Anamorphic prism pairs. [Online]. Available: <https://www.edmundoptics.eu/knowledge-center/application-notes/optics/anamorphic-prism-pairs/>
- [5] Pedrotti³, *Introduction to optics*, 3rd ed. Cambridge MA: Cambridge University Press, 2018.
- [6] F. Inc. Polarization-maintaining fiber (pmf). [Online]. Available: <https://www.fiberlabs.com/glossary/polarization-maintaining-fiber/>
- [7] F. M. J. Cozijn, “Design and construction of a 313 nm diode-laser based system for cooling of trapped beryllium ions,” Master’s thesis, De Boelelaan 1085, Amsterdam, 2016.
- [8] T.W.Hansch and B. Couillaud, “Laser frequency stabilization by polarization spectroscopy of a reflecting reference cavity,” *Optics Communications*, vol. 35, no. 3, pp. 441–444, 1980.
- [9] N. Dubreuil, *Nonlinear Optics - Introduction*, lecture notes ed., 2017.
- [10] R. Paschotta. Brewster’s angle. [Online]. Available: https://www.rp-photonics.com/brewsters_angle.html
- [11] D. Kliukin, Private conversation, April 2022.
- [12] R. Paschotta. Q factor. [Online]. Available: https://www.rp-photonics.com/q_factor.html

Appendices

A Code for analysing beamprofile

```

1 import cv2
2 import sys
3 import os.path
4 import matplotlib.pyplot as plt
5 import pandas as pd
6 from analysis_functions import *
7 from datetime import date
8
9
10 user = 'Thomas'
11 folder_date = '2022_03_02/'
12 image_name = 'ratio_1'
13 extension = '.png'
14
15
16
17
18 if user=='Thomas' :
19     working_directory = 'D:/Study Applied Physics/Jaar 4/AfstudeerStage/
20     Foto Beamprofile/'
21
22 img = cv2.imread(working_directory+folder_date+image_name+extension)[: , : ,
23     1]
24 # img = cv2.imread(folder_date+image_name+extension)[: , : , 1]
25 print(img.shape)
26 pixel_size = 5.86e-6 # Pixel size of MANTA in m
27 # print(img)
28 threshold = 20 # pixel value
29 expected_diameter = 7#mm
30 cropping = 1
31 point_for_interpolation = 500 # number of point use in the interpolation
32     for diag profile (TH analysis only)
33 center = [1165,680]
34 center = None
35 r_mm = 0.0020
36
37
38 x_center = 66
39 y_center = 97
40 p0x = [x_center * pixel_size, r_mm, 100, 10]
41 p0y = [y_center * pixel_size, r_mm, 100, 10]
42 beam = beam_analysis(img, expected_diameter, threshold,
43     point_for_interpolation, p0x, p0y, center)
44 beam.center_seeker()
45 beam.cross_profile()
46 beam.gauss_analysis_(True)
47
48 # let's make a test
49 # let's make another one
50 maximum_value = img.max()
51 my_bbox = {'facecolor': 'red', 'alpha': 0.5, 'pad': 10}
52
53 waist_v = abs(beam.fit_v[1])
54 waist_h = abs(beam.fit_h[1])
55
56 FWHM_v = np.sqrt(2*np.log(2))*waist_v
57 FWHM_h = np.sqrt(2*np.log(2))*waist_h
58
59 string_v = 'Vertical\nw0 = %s mm\nFWHM = %s mm' % (round(waist_v, 3), round

```

```

    (FWHM_v, 3))
56 string_h = 'Horizontal\nw0 = %s mm\nFWHM = %s mm' % (round(waist_h, 3),
    round(FWHM_h, 3))
57
58 X_center = beam.x_center
59 Y_center = beam.y_center
60 Xlim_px = beam.Xlim
61 Ylim_px = beam.Ylim
62 Xlim_mm = beam.Xlim*pixel_size
63 Ylim_mm = beam.Ylim*pixel_size
64
65 LW = 0.5 # Linewidth for plot
66 FS = 10 # Fontsize in textbox
67 print(beam.y_center*pixel_size)
68 fig = plt.figure(image_name, constrained_layout=True).clf()
69 fig = plt.gcf()
70 gs = fig.add_gridspec(4, 4)
71 fig.set_size_inches(10, 5)
72
73 ax1 = fig.add_subplot(gs[0:, 0:2])
74 ax1.imshow(img, cmap='inferno', vmin=0, vmax=240)
75 ax1.set_xlim(Xlim_px)
76 ax1.set_ylim(Ylim_px)
77 ax1.plot(X_center, Y_center, marker='+', markersize=36, color='k')
78 #
79 ax2 = fig.add_subplot(gs[0:2, 2:4])
80 ax2.plot(beam.v_axis-beam.y_center*pixel_size*1e3, beam.v_prof, color='red'
    , linewidth=LW, label='Vertical')
81 ax2.plot(beam.v_axis-beam.y_center*pixel_size*1e3, beam.line_fit_v, color='
    k', linewidth=LW+1, label='Fit')
82 ax2.set_xlim(-expected_diameter/2, expected_diameter/2)
83 ax2.text(0.05, 0.8, string_v, style='italic', transform=ax2.transAxes, bbox
    =my_bbox, fontsize=FS)
84 ax2.legend()
85 #
86 ax3 = fig.add_subplot(gs[2:4:, 2:4])
87 ax3.plot(beam.h_axis-beam.x_center*pixel_size*1e3, beam.h_prof, color='blue
    ', linewidth=LW, label='Horizontal')
88 ax3.plot(beam.h_axis-beam.x_center*pixel_size*1e3, beam.line_fit_h, color='
    k', linewidth=LW+1, label='Fit')
89 ax3.set_xlim(-expected_diameter/2, expected_diameter/2)
90 ax3.text(0.05, 0.8, string_h, style='italic', transform=ax3.transAxes, bbox
    =my_bbox, fontsize=FS)
91 ax3.legend()
92
93 plt.savefig(working_directory+folder_date+image_name+'_analysis.jpeg')
94 # plt.savefig(folder_date+image_name+'_analysis.jpeg')
95 plt.show()

```

Listing 1: *Analysing software made by Dr. Mathieu Collombon*